Foundations and Trends® in
Computer Graphics and Vision
4:3

Kernel Methods in Computer Vision

Christoph H. Lampert

Kernel Methods in Computer Vision

Christoph H. Lampert[1]

[1] *Max Planck Institute for Biological Cybernetics, 72076 Tübingen, Germany,*
`http://www.christoph-lampert.de` `chl@tuebingen.mpg.de`

Abstract

Over the last years, *kernel methods* have established themselves as powerful tools for computer vision researchers as well as for practitioners. In this tutorial, we give an introduction to kernel methods in computer vision from a geometric perspective, introducing not only the ubiquitous support vector machines, but also less known techniques for regression, dimensionality reduction, outlier detection and clustering. Additionally, we give an outlook on very recent, non-classical techniques for the prediction of structure data, for the estimation of statistical dependency and for learning the kernel function itself. All methods are illustrated with examples of successful application from the recent computer vision research literature.

Contents

1

Overview

Computer vision has established itself as a broad subfield of computer science. It spans all areas for building automatic systems that extract information from images, covering a range of applications, from the organization of visual information, over control and monitoring tasks, to interactive and real-time systems for human-computer interaction. Despite this variability, some principled algorithms have emerged over the last years and decades that are useful in many different scenarios and thereby transcend the boundaries of specific applications. One recently very successful class of such algorithms are *kernel methods.* Based on the fundamental concept of defining *similarities* between objects they allow, for example, the prediction of properties of new objects based on the properties of known ones (*classification, regression*), or the identification of common subspaces or subgroups in otherwise unstructured data collections (*dimensionality reduction, clustering*).

1.1 The Goals of this Tutorial

With this tutorial, we aim at giving an introduction to kernel methods with emphasis on their use in computer vision. In the chapter *"Intro-*

duction to Kernel Methods" we use the problem of binary classification with *support vector machines* as introductory example in order to motivate and explain the fundamental concepts underlying all kernel methods. Subsequently, *"Kernels for Computer Vision"* gives an overview of the kernel functions that have been used in the area of computer vision. It also introduces the most important concepts one needs to know for the design of new kernel functions. Although support vector machines (SVMs) are the most popular examples of kernel methods, they are by far not the only useful ones. In the rest of this tutorial, we cover a variety of kernel methods that go beyond binary classification, namely algorithms for *"Multiclass Classification"*, *"Outlier Detection"*, *"Regression"*, *"Dimensionality Reduction"*, and *"Clustering"*. We also include some recent non-standard techniques, namely *"Structured Prediction"*, *"Dependency Estimation"* and techniques for *"Learning the Kernel"* from data. In each case, after introducing the underlying idea and mathematical concepts, we give examples from the computer vision research literature where the methods have been applied successfully. It is our hope that this double-tracked approach will give pointers into both directions, theory and application, for the common benefit of researchers as well as practitioners.

1.2 What this Tutorial is not

This work is not meant to replace an introduction into *machine learning* or generic *kernel methods*. There are excellent textbooks for this purpose, *e.g.* [Schölkopf and Smola, 2002] and [Shawe-Taylor and Cristianini, 2004]. In contrast to a formal introduction, we will sometimes take shortcuts and appeal to the reader's geometric intuition. This is not out of disrespect for the underlying theoretical concepts, which are in fact one of the main reasons why kernel methods have become so successful. It is rather because otherwise we would not be able to achieve our main goal: to give a concise overview of the plethora of kernel methods and to show how one can use them for tackling many interesting computer vision problems.

The limited space that is available in a text like this has another unfortunate consequence: we have to omit a lot of the technical details that most textbooks on kernel method spend many pages on. In particular, we will not cover: *probabilistic foundations*, such as the statistical assumptions on how the data we work with was generated; *statistical learning theory*, including the highly elegant PAC theory and generalization bounds; *optimization theory*, such as dualization and convexity; *numerics*, for example the many methods developed to solve the SVM's and related training problems. All good textbooks on support vector machines and kernel methods cover at least some of these topics, and it is our hope that after reading this introduction into *Kernel Method for Computer Vision*, your interest will be aroused to do further background reading.

2

Introduction to Kernel Methods

To introduce the concept of *kernels*, let us study a toy problem: the classification of fish images. For simplicity, we assume that the images show are only two possible species, *salmon* and *bass*, and that for each fish image we have a way of extracting its dominant color. The task is to come up with a classification rule that can decide for any new fish whether it is a salmon or a bass based on its color. Because we ourselves know nothing about fish, we will not be able to give the system any useful advice. We can, however, make use of a set of example images, called the *training set*, that an expert in fish classification has annotated for us with the correct species labels.

2.1 Notation

To describe the task in mathematical terms, we introduce the following notation:

- *Fish images* are denoted by (color) vectors $x \in \mathbb{R}^d$. In component notation, we write $x = (x^1, \ldots, x^d)$.
- *Class membership* is denoted by a binary variable $y \in \{-1, +1\}$. $y = +1$ means *salmon* and $y = -1$ means *bass*.

- The *training set* of examples for which we have labels is denoted by $X = \{x_1, \dots, x_n\}$.
- The *class labels* of these examples are $Y = \{y_1, \dots, y_n\}$.

From the given data X and Y, we need to determine, or *learn*, a classification function

$$F : \mathbb{R}^d \to \{-1, +1\}, \tag{2.1}$$

that is a function that decides for any new (previously unseen) fish x which species it belongs to.

Clearly, we have infinitely many choices how to parameterize and determine F. In *kernel methods*, we choose F as the *sign*[1] of a linear (strictly speaking affine) function, *i.e.*

$$F(x) = \operatorname{sign} f(x) \tag{2.2}$$

with a *decision function* $f : \mathbb{R}^d \to \mathbb{R}$ that we parameterize as

$$f(x) = a^0 + a^1 x^1 + a^2 x^2 + \dots a^d x^d. \tag{2.3}$$

where $a^0, \dots, a^n$ are the coefficients of f. By writing $w = (a^0, \dots, a^n) \in \mathbb{R}^{d+1}$ and augmenting x with a constant 1 in the first position, $\tilde{x} = (1, x^1, \dots, x^d) \in \mathbb{R}^{d+1}$, we can write f more compactly as

$$f(x) = \langle w, \tilde{x} \rangle \tag{2.4}$$

where $\langle \cdot\,, \cdot \rangle$ denotes the inner product of vectors in $\mathbb{R}^{d+1}$. In the following, we will simplify the notation by assuming that the augmentation is already part of the original feature vector. We will therefore write only x instead of $\tilde{x}$ and work with samples x and weight vectors w in $\mathbb{R}^d$ instead of $\mathbb{R}^{d+1}$. Figure 2.1 illustrates the classification process and how the weight vector w determines the sign of f.

2.2 Linear Classification

Our main question of interest is how one can *learn* a good classification functions F from a set of training examples. Since F is completely

[1] The rare case $f(x) = 0$ can be resolved in an arbitrary way. We just define: $\operatorname{sign} 0 = 1$.

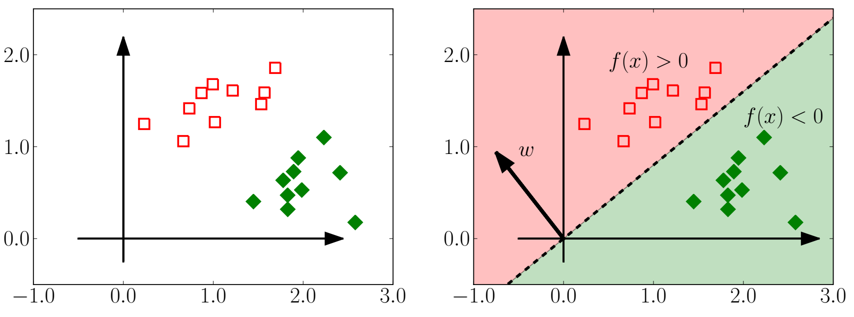

Figure 2.1 Schematic visualization of the *fish* classification task. Left: the training set contains samples of the two classes *salmon* (□) and *bass* (◆). Right: a weight vector w induces a partitioning of the data space by means of a linear decision function $f(x) = \langle w, x \rangle$.

determined by the decision function, the main object of our studies will be f, and we will often also call it the classifier itself. Similarly, because f is determined by w, we will treat the problem of learning f and learning w as equivalent.

In order to derive a learning algorithm, we first characterize the properties that we would expect a good classification function to have:

Definition 2.1 (Correctness). A classifier f is called *correct*, if for all samples in the training set, the labels predicted by f coincide with the training labels, *i.e.*

$$\operatorname{sign} f(x_i) = y_i \qquad \text{for } i = 1, \ldots, n. \tag{2.5}$$

Clearly, *correctness* is a desirable property, because it means that the classifier respects the information given to us in form of the training set. However, there are typically many choices for the weight vector w that lead to *correct* classifiers and not all of them are equally good. This can be seen from Figure 2.2: all three classifiers depicted there classify all training points correctly but, nevertheless, most people would agree that the classifier illustrated in the middle is preferable over the other two, because it appears more *robust* for future decision. We formalize this intuition in the following definition:

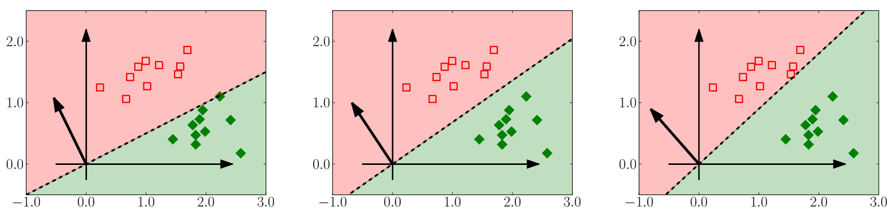

Figure 2.2 *Correctness* (2.5) does not uniquely determine the classifier function: all three classifiers predict the correct labels for all training samples.

Definition 2.2 (Robustness). The *robustness* of a classifier is the largest amount ρ by which we can perturb the sample vectors in the training set such that the prediction of f does not change:

$$\operatorname{sign} f(x_i + \epsilon) = \operatorname{sign} f(x_i) \qquad \text{for } i = 1, \dots, n, \tag{2.6}$$

for all perturbations $\epsilon \in \mathbb{R}^d$ with $\|\varepsilon\| < \rho$.

In contrast to *correctness*, the *robustness* of a classifier is a numerical value: one classifier will be more or less robust than another. As it turns out, we can explicitly calculate the robustness value for any linear classifier with weight vector w for a given training set $\{x_1, \dots, x_n\}$.

Theorem 2.1. The *robustness* of a classifier function $f(x) = \langle w, x\rangle$ is

$$\rho = \min_{i=1,\dots,n} \left| \langle \frac{w}{\|w\|}, x_i \rangle \right| . \tag{2.7}$$

Proof: From

$$f(x_i + \epsilon) = \langle w, x_i + \epsilon\rangle = \langle w, x_i\rangle + \langle w, \epsilon\rangle = f(x_i) + \langle w, \epsilon\rangle \tag{2.8}$$

it follows that

$$f(x_i) - \|w\|\|\varepsilon\| \quad \leq \quad f(x_i + \epsilon) \quad \leq \quad f(x_i) + \|w\|\|\varepsilon\|, \tag{2.9}$$

and by explicitly checking the cases $\varepsilon = \pm\frac{\|\varepsilon\|}{\|w\|} w$ one sees that these inequalities are sharp. In order to ensure Equation (2.6) for all training

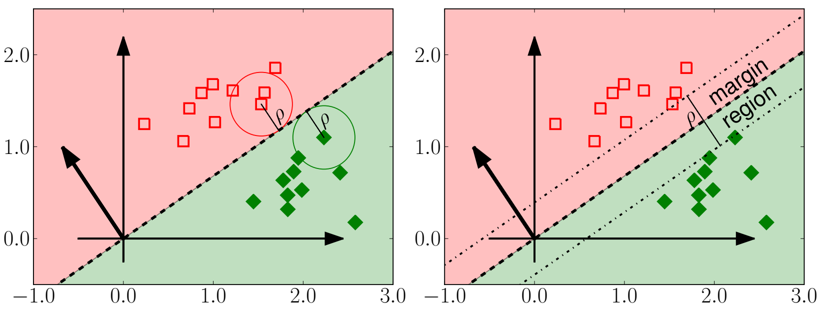

Figure 2.3 The *margin* concept. The *robustness* of a linear classifier, *i.e.* the amount by which training samples can be distorted without them moving across the decision boundary, is identical to the width of the margin, *i.e.* the large region around the decision boundary not containing any training examples.

samples, we must have $|f(x_i)| \geq \|w\|\|\varepsilon\|$ for $i = 1, \dots, n$. Because this inequality holds for all samples, it also holds for the one of minimal score, from which the statement of the theorem follows. $\square$

Geometrically, $\frac{w}{\|w\|}$ is the unit normal vector of the decision hyperplane $H_f = \{f(x) = 0\}$ and $|\langle \frac{w}{\|w\|}, x_i \rangle|$ measures the distance of a sample x_i to H_f, as illustrated in Figure 2.3. The *robustness* of f is therefore identical to half the width of the largest strip around the decision hyperplane that does not contain any training samples, commonly called the *(geometric) margin*.

2.2.1 The Maximum-Margin Classifier

The classifier that combines the properties of *correctness* with maximal *robustness* (or *margin*), is called the *maximum margin classifier*:

Theorem 2.2. Let $X = \{x_1, \dots, x_n\} \subset \mathbb{R}^d$ be a training set with training labels $Y = \{y_1, \dots, y_n\} \subset \{-1, +1\}$. Then the weight vector $w \in \mathbb{R}^d$ of the *maximum margin classifier* is given by the solution to the optimization problem

$$\min_{w \in \mathbb{R}^d} \|w\|^2 \tag{2.10}$$

subject to

$$y_i\langle w, x_i\rangle \geq 1, \qquad \text{for } i = 1, \dots, n. \tag{2.11}$$

Proof: To see that the formulation of Theorem 2.2 indeed describes the *correct* classifier with maximal *robustness*, we first note that the intuitive characterization of a *maximum margin classifier* would be

$$\max_{w\in\mathbb{R}^d} \ \rho \tag{2.12}$$

subject to

$$\rho = \min_{i=1,\dots,n} \left|\langle \frac{w}{\|w\|}, x_i\rangle\right| \tag{2.13}$$

and

$$\operatorname{sign}\langle w, x_i\rangle = y_i, \qquad \text{for } i = 1, \dots, n. \tag{2.14}$$

We can get rid of the minimization in (2.13), by constraining ρ just to be smaller than all $\left|\langle \frac{w}{\|w\|}, x_i\rangle\right|$, for $i = 1, \dots, n$, while at the same time maximizing over it. The optimization problem (2.12)–(2.14) is thus equivalent to solving

$$\max_{w\in\mathbb{R}^d, \rho\in\mathbb{R}^+} \quad \rho \tag{2.15}$$

subject to

$$\left|\langle \frac{w}{\|w\|}, x_i\rangle\right| \geq \rho \qquad \text{for } i = 1, \dots, n, \tag{2.16}$$

and

$$\operatorname{sign}\langle w, x_i\rangle = y_i, \qquad \text{for } i = 1, \dots, n, \tag{2.17}$$

where $\mathbb{R}^+$ stands for the set of positive real numbers. Inserting the equality constraints into the inequalities, and dividing by ρ, we obtain the also equivalent

$$\max_{w\in\mathbb{R}^d, \rho\in\mathbb{R}^+} \quad \rho \tag{2.18}$$

subject to

$$y_i\langle \frac{w}{\rho\|w\|}, x_i\rangle \geq 1, \qquad \text{for } i = 1, \dots, n. \tag{2.19}$$

We now substitute $\tilde{w} = \frac{w}{\rho\|w\|}$. Note that $\tilde{w}$ runs over all of $\mathbb{R}^d$ when $w \in \mathbb{R}^d$ and $\rho \in \mathbb{R}^+$. Using that $\|\tilde{w}\| = \frac{1}{\rho}$, we obtain the equivalent problem

$$\max_{\tilde{w}\in\mathbb{R}^d} \quad \frac{1}{\|\tilde{w}\|} \tag{2.20}$$

subject to

$$y_i\langle \tilde{w}, x_i\rangle \geq 1, \qquad \text{for } i = 1, \dots, n. \tag{2.21}$$

Finally, this is equivalent to the optimization in Theorem 2.2, because maximizing over $\frac{1}{\|\tilde{w}\|}$ has same effect as minimizing over $\|\tilde{w}\|$, or equivalently over $\|\tilde{w}\|^2$. For practical purposes the latter is preferable because it makes the objective function everywhere continuously differentiable.

From the view of optimization theory, solving the problem in Theorem 2.2 numerically is well understood and rather easy: the function we have to minimize is quadratic, *i.e.* in particular differentiable and convex, and all constraints are linear. We can find the globally optimal solution vector in $O(n^2d + n^3)$ operations [Boyd and Vandenberghe, 2004], and there are also many algorithms that find a solution close to the optimal one in much shorter time [Platt, 1999; Joachims, 2006; Chapelle, 2007a; Shalev-Shwartz et al., 2007].

2.2.2 Soft-Margin Classifiers

So far, we have silently assumed that the maximum margin classifier exists. However, depending on the distribution of training samples, this might not be the case. Figure 2.4 (left) illustrates this case: because of an □ outlier between the ◆ samples, no *correct* linear classifier exists that would separate the classes. Mathematically, this means that no weight vector w fulfills all constraints (2.11) at the same time, thereby making the optimization (2.10) impossible to solve. However, we can overcome this problem by making the hard constraints (2.11) into *soft*

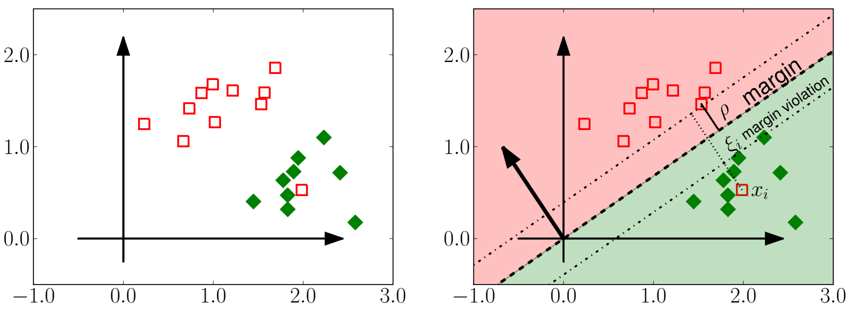

Figure 2.4 Need for soft margin classifiers. Left: because of a □ outlier with in the ◆ class there is no *correct* linear classifier for the training set. Right: We can overcome this problem by also allowing linear classifier that do not classify all training samples correctly, *i.e.* that make some mistakes. The outlier point x_i lies on the incorrect side of the margin region. The amount ξ_i by which this is the case is called its *margin violation*.

constraints, *i.e.* we allow them to be violated, but every violation is penalized by a certain cost term, see Figure 2.4 (right). In terms of an optimization problem, we obtain:

Definition 2.3 (Maximum Soft-Margin Classifier). Let $X = \{x_1, \dots, x_n\} \subset \mathbb{R}^d$ be a training set with training labels $Y = \{y_1, \dots, y_n\} \subset \{-1, +1\}$. Then the weight vector $w \in \mathbb{R}^d$ of the *maximum soft-margin classifier* for any *regularization constant* $C > 0$ is given by the solution to the optimization problem

$$\min_{\substack{w \in \mathbb{R}^d \\ \xi_1,\dots,\xi_n \in \mathbb{R}^+}} \quad \|w\|^2 + \frac{C}{n} \sum_{i=1}^{n} \xi_i \tag{2.22}$$

subject to

$$y_i \langle w, x_i \rangle \geq 1 - \xi_i, \qquad \text{for } i = 1, \dots, n. \tag{2.23}$$

The new variables ξ_i are called *slack variables*. In contrast to the hard-margin case, the *maximum soft-margin classifier* always exists, because we can always fulfill the constraints (2.23) by just making the ξ_i large enough. However, $\xi_i > 0$ means that the sample x_i lies on the wrong

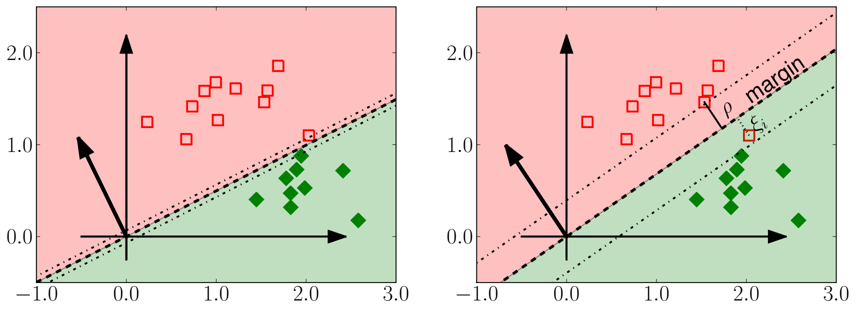

Figure 2.5 *Correctness* vs. *robustness* tradeoff. Even if a *correct* classifier exists (left), we might prefer one that makes some mistakes on the training set (right), if that is much more *robust*.

side of the decision hyperplane (for $\xi_i > 1$), or at least inside of the margin region (for $0 < \xi_i \leq 1$). Therefore, we would like the ξ_i to be as small as possible. This is achieved by including the new term $\frac{C}{n} \sum_i \xi_i$ into the minimization of (2.22).

The constant C in Definition 2.3, allows us to trade off between *correctness* and *robustness* of the classifier. This is often a desirable property, as can be seen in Figure 2.5: even in situations where a *correct* classifier exists, *i.e.* a solution to the problem (2.10), we might want to allow for some outliers and search for a *soft-margin solution* instead. This, one would hope, will make the resulting classifier more robust for the correctly classified samples and thus make fewer mistakes on future data samples. The *regularization constant* C allows us to control this behavior: if C is very small, margin violations matter hardly at all, and the optimization concentrates on minimizing $\|w\|^2$, *i.e.* on achieving a large margin area. Alternatively, if C is very large, every violation of a margin constraint will be penalized heavily, and, if possible, the soft-margin classifier will be very close or identical to the hard-margin classifier. Note that in most cases the question whether more or less regularization is required cannot be answered *a priori*. It depends on the data set what value of C results in the best generalization performance. Therefore, one typically has to use a validation set

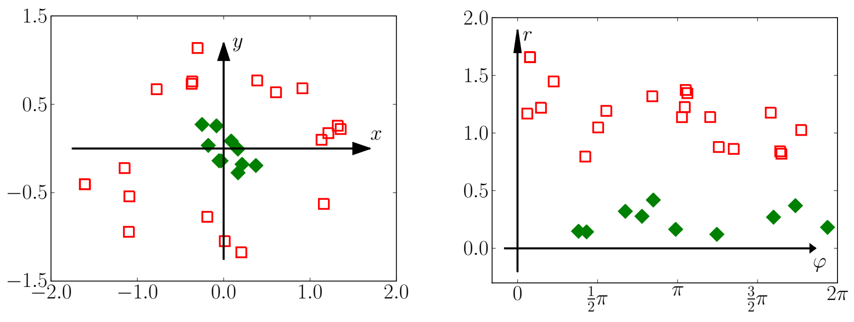

Figure 2.6 Non-linear preprocessing. Left: for some distribution of training samples, no linear classifier will yield satisfactory results. Right: linear classification can be possible again if we first transform the samples into a new coordinate system, here from Cartesian to polar coordinates: $(x, y) \mapsto (\theta, r)$.

or perform cross-validation to determine the C parameter[2].

2.3 Non-linear Classification

In some situations, there is no hope for any good linear classifier, even if we allow for margin violations. An example is depicted in Figure 2.6 (left): no linear classifier is going to achieve satisfactory performance. Consequently, many ideas for non-linear classification have been developed, often based on the concept of combining the decisions of many linear classifiers into one non-linear one, *e.g. decision trees* [Quinlan, 1986; Breiman, 1998], *multi-layer perceptrons* [Bishop, 1995; Hinton et al., 2006] or *boosting* [Schapire and Freund, 1997]. In *kernel methods* we follow a different paradigm: first, we apply a non-linearly transformation to the data, and afterwards, we again learn a single linear classifier to the resulting transformed dataset. By choosing a suitable coordinate transformation, a difficult non-linear problem can be become an easy linear one, as is illustrated in Figure 2.6 (right).

This intuition leads to a natural extension of linear classifiers to *generalized linear classifiers*:

---

[2] Note that the objective function (2.22) is monotonously increasing in C. Optimizing over this value is therefore not an option in order to determine C.

Definition 2.4 (Generalized Linear Max-Margin Classifier). Let $X = \{x_1, \dots, x_n\} \subset \mathbb{R}^d$ be a training set with training labels $Y = \{y_1, \dots, y_n\} \subset \{-1, +1\}$, and let $\varphi : \mathbb{R}^d \to \mathbb{R}^m$ be a (possibly non-linear) map. Then the *generalized linear max-margin classifier* for any regularization constant $C > 0$ is given by $F(x) = \operatorname{sign} f(x)$ for

$$f(x) = \langle w, \varphi(x) \rangle, \tag{2.24}$$

where $w \in \mathbb{R}^m$ is the solution to the optimization problem

$$\min_{\substack{w \in \mathbb{R}^m \\ \xi_1, \dots, \xi_n \in \mathbb{R}^+}} \|w\|^2 + \frac{C}{n} \sum_{i=1}^{n} \xi_i \tag{2.25}$$

subject to

$$y_i \langle w, \varphi(x_i) \rangle \geq 1 - \xi_i, \qquad \text{for } i = 1, \dots, n. \tag{2.26}$$

In other words, we find the best linear classifier for the transformed dataset $\{\varphi(x_1), \dots, \varphi(x_n)\} \subset \mathbb{R}^m$. This makes the *generalized linear max-margin classifier* f a linear function in w and $\varphi(x)$. However, if φ is non-linear, f will be non-linear with respect to the original variable x.

2.3.1 Example Feature Mappings

Definition 2.4 does not put any restrictions on the feature map $\varphi : \mathbb{R}^d \to \mathbb{R}^m$. However, the performance of the resulting classifier will, of course, depend on its choice. Possible feature maps that have proved to be useful for vectorial data are:

- Polar coordinates for $(x, y) \in \mathbb{R}^2$:

$$\varphi : \begin{pmatrix} x \\ y \end{pmatrix} \mapsto \begin{pmatrix} \sqrt{x^2 + y^2} \\ \arctan \frac{y}{x} \end{pmatrix}$$

- m-th degree polynomials for $x = (x_1, \dots, x_d) \in \mathbb{R}^d$:

$$\varphi : x \mapsto \left(1, x_1, \dots, x_d, x_1^2, \dots, x_d^2, \dots, x_1^m, \dots, x_d^m\right)$$

- Prototype distance map for $x \in \mathbb{R}^d$:

$$\varphi : x \mapsto \Big(\|x - p_1\|, \dots, \|x - p_N\| \Big)$$

  where $\{p_1, \dots, p_N\} \subset \mathbb{R}^d$ is a set of N prototype vectors.

As one can see from the polynomials and from the distance map, the dimensionality of the target space can be much larger than that of the original space. This gives a generalized linear classifier with weight vector in $\mathbb{R}^m$ more flexibility than the original linear one in $\mathbb{R}^d$, and one can hope for better classification accuracy. However, by mapping the data into a very high-dimensional space one would expect that the memory usage and the runtime required to solve the optimization problem will increase. It is one of the most interesting properties of kernel method that these worries are baseless, as we will see in the following.

2.4 The Representer Theorem

The weight vector w of a generalized linear classifier with preprocessing map $\varphi : \mathbb{R}^d \to \mathbb{R}^m$ has m components that need to be determined. However, it follows from the following *Representer Theorem* that w cannot be arbitrary, but it lies in a subspace of $\mathbb{R}^m$ of dimension n or less, where n is the number of training samples.

Theorem 2.3 (Representer Theorem). The minimizing solution w to the optimization problem (2.25) can always be written as

$$w = \sum_{j=1}^{n} \alpha_j \varphi(x_j) \qquad \text{for coefficients } \alpha_1, \dots, \alpha_n \in \mathbb{R}. \tag{2.27}$$

Proof: Although the Representer Theorem is of central important in the area of kernel methods, its proof is relatively elementary. Let V denote the span of the vectors $\varphi(x_1), \dots, \varphi(x_n)$, *i.e.* the subspace of all vectors that can be expressed as linear combinations $\sum_j \alpha_j \varphi(x_j)$. Let $w \in \mathbb{R}^m$ be the solution vector the optimization problem (2.25). To prove the theorem, we then have to show that $w \in V$.

Because V is a finite-dimensional subspace, every vector in $\mathbb{R}^m$ has a unique decomposition into one component from V and one from its orthogonal complement $V^\perp = \{u \in \mathbb{R}^m : \langle u, v\rangle = 0 \text{ for all } v \in V\}$. Let $w = w_V + w_{V^\perp}$ be this decomposition for w. We then observe that $\langle w_{V^\perp}, \varphi(x_i)\rangle = 0$ for all $i = 1, \ldots, n$, because $\varphi(x_i) \in V$. Therefore, $\langle w, \varphi(x_i)\rangle = \langle w_V, \varphi(x_i)\rangle$, which shows that w_V fulfills the inequality constraints (2.34) with same values for the slack variables ξ_i as w does. At the same time, $\|w\|^2 = \|w_V\|^2 + \|w_{V^\perp}\|^2$, with no cross-terms appearing because $\langle w_V, w_{V^\perp}\rangle = 0$. Now $w_{V^\perp} = 0$ follows by contradiction: $\|w_{V^\perp}\| > 0$ would imply that $\|w_V\|^2$ is strictly smaller then $\|w\|^2$, but w was assumed to be solution minimizing (2.25). Consequently, we have $w_{V^\perp} = 0$, which implies $w = w_V \in V$ and proves the theorem. □

The first important consequence of the Representer Theorem is the possibility to rewrite the problem of learning a generalized linear classifier from an m-dimensional optimization problem into an n-dimensional one. For this, we insert the representation $w = \sum_{j=1}^n \alpha_j \varphi(x_j)$ into (2.25) and (2.26). Subsequently, we can optimize over $(\alpha_1, \ldots, \alpha_n) \in \mathbb{R}^n$ instead of $w \in \mathbb{R}^m$. Using the linearity of the inner product, we obtain

$$\min_{\substack{\alpha_1,\ldots,\alpha_n \in \mathbb{R}\\ \xi_1,\ldots,\xi_n \in \mathbb{R}^+}} \quad \sum_{i,j=1}^n \alpha_i \alpha_j \langle\, \varphi(x_i), \varphi(x_j)\,\rangle + \frac{C}{n}\sum_{i=1}^n \xi_i \tag{2.28}$$

subject to

$$y_i \sum_{j=1}^n \alpha_j \langle\, \varphi(x_j), \varphi(x_i)\,\rangle \geq 1 - \xi_i, \qquad \text{for } i = 1, \ldots, n, \tag{2.29}$$

and the generalized linear decision function (2.24) becomes

$$f(x) = \sum_{j=1}^n \alpha_j \langle\, \varphi(x_j), \varphi(x)\,\rangle. \tag{2.30}$$

A special property of this problem is, that the coefficient vector $(\alpha_j)_{j=1,\ldots,n}$ will be *sparse*, *i.e.* most of the coefficients α_j will have a value of 0 [Schölkopf and Smola, 2002]. This simplifies and speeds up the calculation of the decision function (2.30). The training examples x_j with non-zero coefficients α_j are often called *support vectors*, because they support the decision hyperplane.

2.5 Kernelization

The Representer Theorem allows us to reduce[3] the size of the optimization problem for finding the generalized max-margin classifier. However, calculating and storing $\{\varphi(x_1), \dots, \varphi(x_n)\}$ could still require a lot of memory. We can avoid this bottleneck as well, by observing that the optimization problem (2.28) contains the transformed features $\varphi(x_i)$ only pairwise in inner products, *i.e.* as part of expressions $\langle \varphi(x_i), \varphi(x_j) \rangle$ for $i, j = 1, \dots, n$. Because of symmetry, this quantity has $\frac{n(n+1)}{2}$ unique values. If we precompute and store these, we do not need to store the nm entries of the vectors $\varphi(x_i)$ anymore.

More generally, we can define the *kernel function* $k : \mathbb{R}^d \times \mathbb{R}^d \to \mathbb{R}$ of φ by the identity

$$k(x, x') = \langle \varphi(x), \varphi(x') \rangle. \tag{2.31}$$

Rewriting the problem (2.28) by means of this notation, we obtain the optimization problem for the generalized linear max-margin classifier in *kernelized* form, often called **support vector machine (SVM)**.

Theorem 2.4 (Support Vector Machine).
Let $X = \{x_1, \dots, x_n\} \subset \mathbb{R}^d$ be a training set with labels $Y = \{y_1, \dots, y_n\} \subset \{-1, +1\}$, let $k : \mathbb{R}^d \times \mathbb{R}^d \to \mathbb{R}$ be a kernel function, and let $C > 0$. Then the decision function of the *kernelized* max-margin classifier is given by

$$f(x) = \sum_{i=1}^{n} \alpha_i k(x_i, x) \tag{2.32}$$

for coefficients $\alpha_1, \dots, \alpha_n$ obtained by solving

$$\min_{\substack{\alpha_1,\dots,\alpha_n \in \mathbb{R} \\ \xi_1,\dots,\xi_n \in \mathbb{R}^+}} \quad \sum_{i,j=1}^{n} \alpha_i \alpha_j k(x_i, x_j) + \frac{C}{n} \sum_{i=1}^{n} \xi_i, \tag{2.33}$$

[3] It is only a reduction if the dimension m of the feature space is larger than the number of training examples n, but this is the case for most of the non-linear feature maps commonly used in computer vision.

subject to

$$y_i \sum_{j=1}^{n} \alpha_j k(x_j, x_i) \geq 1 - \xi_i, \qquad \text{for } i = 1, \dots n. \tag{2.34}$$

Note that many equivalent formulation exist, which can be found in the SVM literature, *e.g.* as an unconstrained optimization problem with Hinge loss [Chapelle, 2007b], in the Lagrangian dual domain [Schölkopf and Smola, 2002], or as a geometric problem of finding points on reduced convex hulls [Bennett and Bredensteiner, 2000].

2.5.1 Why kernelize?

At first sight, introducing $k(x, x')$ has not improved our situation. Instead of calculating $\langle\, \varphi(x_i), \varphi(x_j)\,\rangle$ for $i, j = 1, \dots, n$, we have to calculate $k(x_i, x_j)$, which has exactly the same values. However, there are two potential reasons why the kernelized setup can be advantageous:

Reason 1: Speed. We might find an expression for $k(x_i, x_j)$ that is faster to calculate than forming $\varphi(x_i)$ and then $\langle \varphi(x_i), \varphi(x_j)\rangle$.

As an example, we look at a $2nd$-order polynomial feature map (for simplicity only for $x \in \mathbb{R}^1$). Calculating the feature map

$$\varphi : x \mapsto (1, \sqrt{2}x, x^2) \in \mathbb{R}^3 \tag{2.35}$$

requires 2 multiplication per sample, which makes $2n$ for the whole training set. Subsequently, each inner product requires 5 operations (3 multiplication and 2 additions), which sums up to $\frac{5}{2}n(n+1)$ for the $n(n+1)/2$ unique elements of $\langle \varphi(x_i), \varphi(x_j)\rangle$ for $i, j = 1, \dots, n$. In total, we therefore require $\frac{5}{2}n^2 + \frac{9}{2}n$ operations before we can start the optimization.

The use of a kernel function allows us to simplify the expressions before starting the evaluation:

$$\begin{aligned} k(x, x') = \langle\, \varphi(x), \varphi(x')\rangle &= \langle (1, \sqrt{2}x, x^2)^t\,, (1, \sqrt{2}x', x'^2)^t\,\rangle && (2.36) \\ &= 1 + 2xx' + x^2x'^2 && (2.37) \\ &= (1 + xx')^2 && (2.38) \end{aligned}$$

Therefore, each evaluation of $k(x_i, x_j)$ requires only 3 operations (2 multiplications and 1 addition) for a total of $\frac{3}{2}n^2 + \frac{3}{2}n$ operations for all unique entries $k(x_i, x_j)$ for $i, j = 1, \dots, n$. Thus, we were able to save more than 40% of operations by the kernelization.

Reason 2: Flexibility. We can construct functions $k(x, x')$, for which we *know* that they corresponds to inner products after some feature mapping φ, but we do not know how to compute φ.

This slightly non-intuitive statement is a consequence of the second important theorem in kernel methods:

Theorem 2.5 (Mercer's Condition). Let $\mathcal{X}$ be non-empty set. For any positive definite kernel function $k : \mathcal{X} \times \mathcal{X} \to \mathbb{R}$, there exists a Hilbert space $\mathcal{H}$ and a feature map $\varphi : \mathcal{X} \to \mathcal{H}$ such that

$$k(x, x') = \langle \varphi(x), \varphi(x') \rangle_{\mathcal{H}} \tag{2.39}$$

where $\langle \cdot\,, \cdot \rangle_{\mathcal{H}}$ denotes the inner product in $\mathcal{H}$.

The proof consists of an explicit construction, see *e.g.* [Schölkopf and Smola, 2002]. Before discussing the consequences of Theorem 2.5, we give the missing definitions of *positive definite kernel* and *Hilbert space.*

Definition 2.5 (Positive Definite Kernel Function). Let $\mathcal{X}$ be a non-empty set. A function $k : \mathcal{X} \times \mathcal{X} \to \mathbb{R}$ is called **positive definite kernel function**, if the following conditions hold:

- k is symmetric, *i.e.* $k(x, x') = k(x', x)$ for all $x, x' \in \mathcal{X}$.
- For any finite set of points $x_1, \dots, x_n \in \mathcal{X}$, the *kernel matrix*

  $$K_{ij} = \big(k(x_i, x_j)\big)_{i,j} \tag{2.40}$$

  is positive semidefinite, *i.e.* for all vectors $t \in \mathbb{R}^n$

  $$\sum_{i,j=1}^{n} t_i K_{ij} t_j \geq 0. \tag{2.41}$$

Because all kernels that we study in the following are in fact *positive definite*, we will often just say *kernel* as shorthand for *positive definite kernel function.*

Definition 2.6 (Hilbert Space). A vector space $\mathcal{H}$ is called *Hilbert space*, if the following conditions hold:

- $\mathcal{H}$ is equipped with an inner product
$$\langle \cdot\,, \cdot \rangle_{\mathcal{H}} : \mathcal{H} \times \mathcal{H} \to \mathbb{R}. \tag{2.42}$$
- $\mathcal{H}$ is complete under the induced norm $\|v\|_{\mathcal{H}} = \sqrt{\langle v\,, v \rangle_{\mathcal{H}}}$, *i.e.* all Cauchy sequences of elements in $\mathcal{H}$ converge to a limit that lies in $\mathcal{H}$.

For our purposes, the *completeness* property is of less importance, but the existence of an inner product is crucial because we want to use the kernel function k as a replacement for the evaluation of $\langle \cdot\,, \cdot \rangle_{\mathcal{H}}$.

2.5.2 Classification for non-vectorial data

Theorem 2.5 has some fundamental consequences. In particular, it states that we can use *any* function $k : \mathbb{R}^d \times \mathbb{R}^d \to \mathbb{R}$ and use it in the context of the support vector machine classifier (2.33), as long as k is a positive definite kernel function[4]. The resulting optimization will always correspond to a generalized linear max-margin classifier based on a feature map φ from $\mathbb{R}^d$ into a suitable feature space $\mathcal{H}$. Note that φ and $\mathcal{H}$ are both defined only *implicitly*, *i.e.* we know that they exist, but we might not be able to calculate them. In particular, $\mathcal{H}$ is typically very high or even infinite dimensional, but this does not have to bother us, because our only contact with $\mathcal{H}$ is through its inner product $\langle \cdot\,, \cdot \rangle_{\mathcal{H}}$, and that we can calculate using k.

Furthermore, because the conditions of Theorem 2.5 are not restricted to input domains $\mathbb{R}^d$, we can extend our notion of generalized linear classifiers to *arbitrary input sets* $\mathcal{X}$, as long as we can define a kernel for their elements. We will later see examples of such kernels.

[4] In the previous section we have formulated and proved the Representer Theorem only for feature maps $\varphi : \mathbb{R}^d \to \mathbb{R}^m$. However, it holds in much more general settings, with almost identical proof, see *e.g.* [Schölkopf and Smola, 2002]

2.6 Constructing Kernel Functions

Although Definition 2.5 of *positive definite kernel functions* is relatively simple, it is difficult to check the criteria in practice for a given function $k : \mathcal{X}\times\mathcal{X} \to \mathbb{R}$, because condition (2.41) is a statement about the values of k on arbitrarily large finite subsets of $\mathcal{X}$.

However, it is relatively easy to *construct* functions k that are positive definite kernels, by making use of the following principles:

1) We can *construct kernels from scratch*:

- For any $\varphi : \mathcal{X} \to \mathbb{R}^m$, $k(x, x') = \langle\varphi(x), \varphi(x')\rangle$ is a kernel.
- If $d : \mathcal{X} \times \mathcal{X} \to \mathbb{R}$ is a *distance function*, *i.e.*
  - $d(x, x') \geq 0 \quad$ for all $x, x' \in \mathcal{X}$,
  - $d(x, x') = 0 \quad$ only for $x = x'$,
  - $d(x, x') = d(x', x) \quad$ for all $x, x' \in \mathcal{X}$,
  - $d(x, x') \leq d(x, x'') + d(x'', x') \quad$ for all $x, x', x'' \in \mathcal{X}$,

  then $k(x, x') = \exp(-d(x, x'))$ is a kernel.

2) We can *construct kernels from other kernels*:

- If k is a kernel and $\alpha \in \mathbb{R}^+$, then $k + \alpha$ and αk are kernels.
- if k_1, k_2 are kernels, then $k_1 + k_2$ and $k_1 \cdot k_2$ are kernels.

2.6.1 Kernel Examples

Using the rule for kernel combinations, we can check that the following functions are positive definite kernels for vectors in $\mathbb{R}^d$:

- any linear combination $\sum_j \alpha_j k_j$ with k_j kernels and $\alpha_j \geq 0$,
- any polynomial kernel $k(x, x') = (1 + \langle x, x'\rangle)^m$, $m \in \mathbb{N}$,
- the Gaussian kernel $k(x, x') = \exp\left(-\frac{\|x-x'\|^2}{2\sigma^2}\right)$ with $\sigma > 0$.

The following are examples of kernels for other domains $\mathcal{X}$:

- for d-bin histograms h, h' [Odone et al., 2005][5]:

$$k(h, h') = \sum_{i=1}^{d} \min(h_i, h'_i)$$

[5] The *histogram intersection kernel* is another example of a kernel for which we can derive

- for probability densities p, p': $k(p, p') = \exp(-JS(p, p'))$, where
$$JS(p,p') = \frac{1}{2}\int_{\mathbb{R}} p(x)\log\frac{p(x)}{\frac{1}{2}(p(x)+p'(x))} + p'(x)\log\frac{p'(x)}{\frac{1}{2}(p(x)+p'(x))}$$
is the *Jensen-Shannon divergence* [Hein and Bousquet, 2005],
- for *strings* s, s': $k(s, s') = \exp(-D(s, s'))$, where $D(s, s')$ is the *edit distance* [Gusfield, 1997].

On the other hand, one can show that the function

- $\tanh(a\langle x, x'\rangle + b)$,

which is a popular *transfer function* for artificial neural networks, is not a positive definite kernel.

2.7 Choosing the Kernel Function and its Parameters

From the previous section we saw many possibilities how to construct kernels. Most of these are in fact parameterized families of kernels: each choice of the order m for a polynomial kernels, or of the bandwidth $\sigma > 0$ for a Gaussian kernel, gives rise to a legitimate kernel function. However, simply from the existence of an induced Hilbert space and feature map we cannot infer that the resulting generalized linear classifier will achieve high accuracy.

The two most important questions for practitioners in kernel methods are therefore: *What kernel function should one use?* and *How should one set the kernel parameters?* Unfortunately, there is no universally correct answer, and typically, the best solution is to try different

an explicit feature map φ, but which is much faster to compute in functional form than as an inner product: assume histograms $h = (h_1, \dots, h_d)$ with positive integer entries (*e.g.* raw counts) that sum at most to N. Then the feature map

$$\psi(h_i) = (\underbrace{1,\dots,1}_{h_i \text{ entries}}, \underbrace{0,\dots,0}_{N-h_i \text{ entries}}), \tag{2.43}$$

i.e. a fixed length unary coding of the histogram, turns each summand into an inner product $\min(h_i, h'_i) = \langle\psi(h_i), \psi(h'_i)\rangle$. Concatenating these, we obtain a feature map $\varphi(h) = (\psi(h_1), \dots, \psi(h_d))$ such that $k(h, h') = \langle\varphi(h), \varphi(h')\rangle$. However, calculating $k(h, h')$ directly requires $O(d)$ operations whereas by means of $\varphi(h)$ it is at least $O(dN)$.

possibilities and evaluate the resulting classifiers on a validation set or by cross-validation [Efron and Gong, 1983; Kohavi, 1995]. If that is not possible, one can rely on the following heuristic to guide in the decision:

- A good kernel should have *high values* when applied to two similar objects, and it should have *low values* when applied to two dissimilar objects[6].

There reasoning behind this statement can be seen from looking at a binary classification scenario and imagining a hypothetical *perfect feature function*, $\varphi : \mathcal{X} \to \mathbb{R}$ that fulfills $\varphi(x) = +1$ for every sample of one class and $\varphi(x) = -1$ for samples of the other class. The resulting kernel function $k(x, x') = \varphi(x)\varphi(x')$ will have the value $+1$ whenever x and x' belong to the same class, and -1 otherwise.

2.7.1 Numerical Heuristics

For generalized Gaussian kernels that have the form

$$k(x, x') = \exp(-\gamma\, d^2(x, x')),$$

where d is a distance function, a *rule of thumb* for setting γ is

$$\frac{1}{\gamma} \approx \operatorname*{median}_{i,j=1,\ldots,n} d(x_i, x_j). \tag{2.44}$$

This rule is based on the fact that the squared exponential curve has its point of strongest decline where the exponent is -1. Rescaling the distances in a way that brings the median of d to this point ensures that there will be roughly the same number of *similar* as *dissimilar* samples pairs. More involved variants of this rule include, for example, an additional scale factor that reflects the potential class imbalance. For other kernels based on the exponential function, similar rules of thumb are used, typically using the inverse of the median or of the mean of the exponent as scaling factor, see *e.g.* [Zhang et al., 2007].

[6] Because of this property, it is natural to think of kernels also as a special class of *similarity measures*.

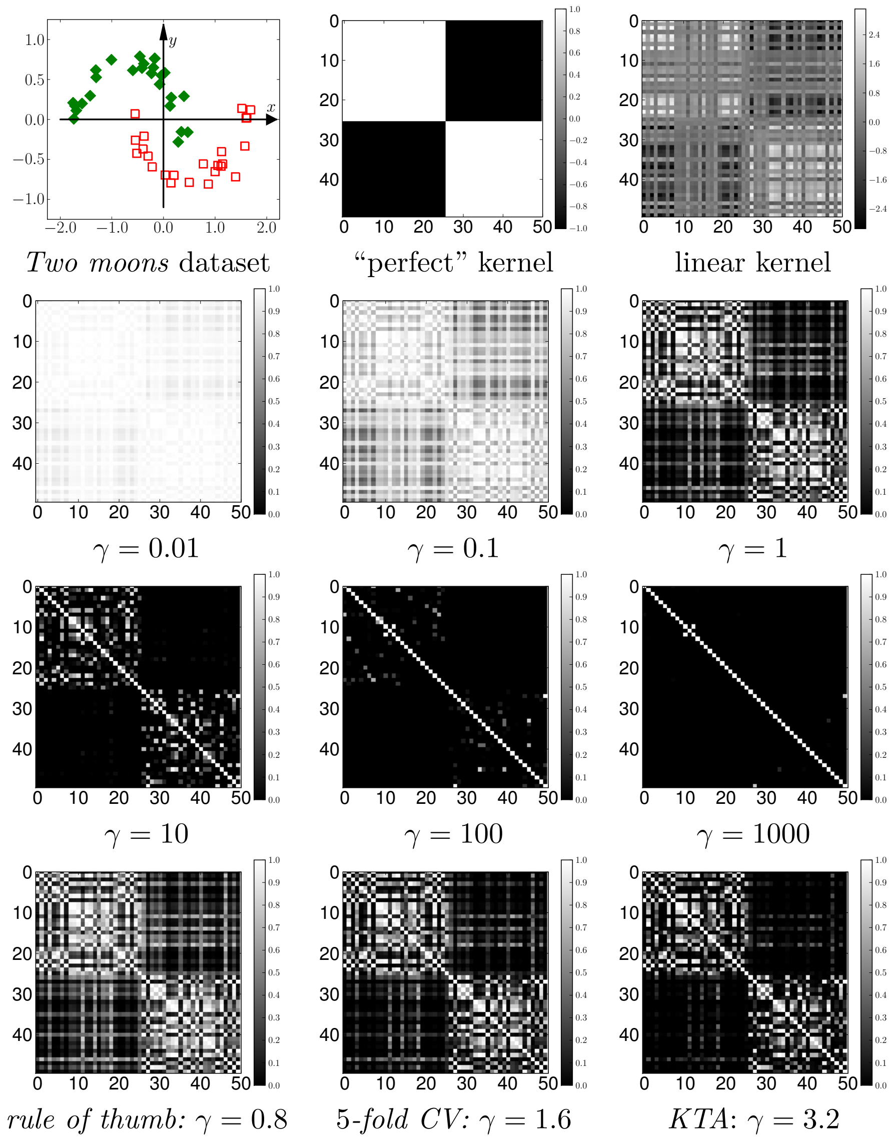

Figure 2.7 Kernel and parameter selection for a *Two Moons* dataset (top row, left). Kernel matrices (in reading order): a hypothetical “perfect” kernel would show a block structure with respect to the classes. A *linear kernel* achieves this only for some samples. *Gaussian* kernels with too small scale parameter ($\gamma \in \{0.01, 0.1\}$) cause almost all samples to be very similar to each other, even if they are from different classes. Between $\gamma = 1$ and $\gamma = 10$, the classes form visible blocks. Larger values ($\gamma \in \{100, 1000\}$) cause most samples to be only similar to themselves. The *rule of thumb* Eq. (2.44) results in a kernel with reasonable block structure, but *cross-validation (CV)* and *kernel target alignment (KTA)* (that will be introduced in the chapter “Learning the Kernel”) yield slightly more pronounced ones.

2.7.2 Visual Heuristics

Figure 2.7 illustrates another heuristic: a kernel function chosen is good for a dataset $\{x_1, \ldots, x_n\}$ if the kernel matrix

$$K = k(x_i, x_j)_{i,j=1,\ldots,n}$$

has a *visible block structure* with respect to the classes in the dataset. Again, this is based on the intuition that the kernel values within a class should be large and between classes should be small. A less heuristic treatment of the question how to choose a kernel function and its parameters can be found in the chapter *Learning the Kernel*.

3

Kernels for Computer Vision

Images and videos are data sources with very special characteristics: because each pixel represents a measurement, images are typically very high dimensional. At the same time, images have properties that we do not observe in arbitrary vector representations, *e.g.* strong correlations between neighboring pixels. Therefore, computer vision researchers have directed special attention on finding good data representations and algorithms that allow one to tackle problems, such as

- **Optical character recognition**: classify images of handwritten or printed letters or digits,
- **Object classification**: classify natural images according to which objects they contain,
- **Action recognition**: classify video sequences by what events occur in them,
- **Image segmentation**: partition an image into the exact subregions that correspond to different image aspects, *e.g.* objects or scenery,
- **Content Based Image retrieval**: find images in an image collection or database that are most similar to a query image.

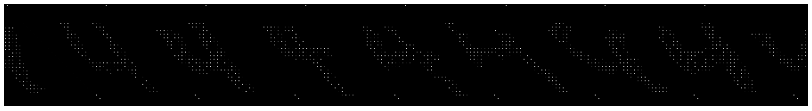
Figure 3.1 Image variability: Humans easily identify all these images as the handwritten digit 4 despite the differences in visual appearance and large Euclidean distance.

Kernel methods have proved successful in all of these areas, mainly because of their interpretability and flexibility: in constructing a kernel function one can incorporate knowledge that humans have about the problem at hand. Typically, this leads to improved performance compared to pure black-box methods that do not allow the integration of prior knowledge. Once a promising kernel function has been designed, it can be re-used in any kernel-based algorithm, not just in the context it was originally designed for. This gives researchers as well as practitioners a large pool of established kernel functions to choose from, thereby increasing the chances of finding a well-performing one.

In the following, we introduce some of the existing kernels with the assumptions they are based on, and we discuss their applicability to practical computer vision tasks.

3.1 Designing Image Kernels

The easiest way to treat images is as vectors of pixel intensities. Images of size $N \times M$ pixels with values in $[0, 255]$ or $[0, 1]$ become vectors $x \in \mathbb{R}^{NM}$, and we can apply any kernel for vectorial data, *e.g.* linear or Gaussian. In the case of binary images $x \in \{0, 1\}^{NM}$, polynomial kernels have also proven successful. Clearly, because these kernels can only compare vectors of identical lengths, all images to be used for learning need to be of the same size.

Unfortunately, treating images directly as vectors has some non-intuitive consequences. In particular, pixel-wise comparisons are typically *too strict*: images that humans would consider very similar can occur very different when compared using a pixel-wise distance measure such as the *Euclidean* norm, see Figure 3.1. The reason for this is that the pixel representation lacks many *invariances* that are implicitly used in the human judgement of image similarity. *Translations*, (small) *rotations*, (small) *changes in size*, *blur*, *brightness* and *contrast* are examples of factors that humans typically consider irrelevant when judging if two images show the same object. Other sources of invariance are domain dependent, *e.g.* the *stroke width* for character images or the *illuminant color* for natural scenes.

Ultimately, many problems in the design of useful image kernels can be reduced to the decision, which invariances to incorporate into the kernel construction and how to do so efficiently.

3.2 Incorporating Invariance

The need for incorporating image invariances into kernel methods can also be understood from looking at the SVM decision function $f(x) = \sum_i \alpha_i k(x_i, x)$ for a test sample x. Only if $k(x_i, x)$ is large enough for some training samples x_i can the decision score be significantly different from 0. Otherwise $f(x) \approx 0$, *i.e.* the test sample lies very close to the decision hyperplane and the classifier becomes unreliable. For the commonly used Gaussian kernel, $k(x, x_i)$ is significantly larger than 0 only for samples x_i that are similar enough to x in the Euclidean norm. However, as discussed above, even images that are visually similar to x might have a large Euclidean distance, in which case they will not contribute to the decision function. Vice versa, a test sample x that is classified reliably by f might be classified unreliably or even incorrectly when undergoing only a slight geometric distortion.

Because of this phenomenon, kernels based on the Euclidean distance between the pixel representations of images can rarely be applied successfully for computer vision task. Several methods to overcome this limitation have been developed, which can be categorized into four main approaches:

(1) extending the training set,
(2) image normalization,
(3) invariant kernel functions,
(4) invariant representations.

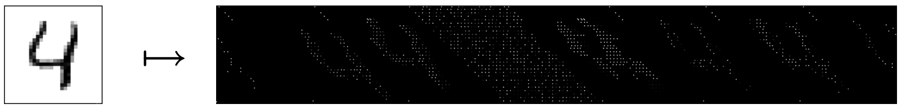

Figure 3.2 Invariance through *virtual samples*: for each training image (left), additional *synthetic* training images (right) are generated and to the training set, *e.g.* through *translation*, *rotation*, *noise*, *blur*, *contrast change*, *stroke width increase* and *thinning.*

3.2.1 Extending the Training Set

We saw above that achieving good classification performance with a Gaussian or similar kernel requires us to have at least some training examples that are close to the test samples with respect to the chosen similarity measure. The easiest way to increase the chances for this is by using more and more training samples until the whole data space is covered densely enough. In practice, the amount of training samples is usually limited, but we can achieve a similar effect by introducing *artificial* or *virtual* training samples [Decoste and Schölkopf, 2002][1]: for each original training sample we create multiple copies that are distorted with the transformations against which we would like the system to be invariant, *e.g.* translations, rotations and noise, see Figure 3.2. Each new sample is assigned the same training label as the original it was created from and added to the training set.

Advantages: The learning method becomes more invariant to image distortions, because more prototypes are available, in particular also distorted versions.

Disadvantages: We need a *generating procedure* that can create distorted versions of the training images. The larger the sample set, the more time and storage is typically required to train and apply the algorithm.

[1] This trick is not an invention of kernel methods. Similar ideas have been used previously under the name of *jittering e.g.* to train neural networks [Linden and Kindermann, 1989; Sietsma and Dow, 1991] and decision trees [Baird, 1993].

Conclusion: Use virtual samples if the training set is small and if invariance against known sources of distortion is required that can be simulated computationally.

3.2.2 Image Normalization

A lot of image variability can be avoided by *normalizing* training and test images before applying the kernel. A typical procedure for this is the *resizing* of all images to a fixed size. *Brightness* and *contrast normalization* are per-pixel operations that can be applied to reduce unwanted variations in the data range between different images. Setting

$$\hat{x} = \frac{x - x^{min}}{x^{max} - x^{min}}, \tag{3.1}$$

where x^{min} and x^{max} are the minimal and maximal grayvalue of the image $x \in \mathbb{R}^{NM}$, the gray values of the resulting image $\hat{x}$ will always cover the full range $[0,1]$, see Figure 3.3(a). For color images, contrast normalization can be applied to each color channel separately.

To make small images or image areas invariant against geometric transformations like *translation* and *rotation*, normalization to a uniform frame can be applied, *e.g.* by moment matching. We calculate the *first* and *second order moment* for an image x with pixels $x[i,j]$:

$$m_x = \frac{1}{m}\sum_{i,j} i\, x[i,j], \qquad m_y = \frac{1}{m}\sum_{i,j} j\, x[i,j], \tag{3.2}$$

$$m_{xx} = \frac{1}{m}\sum_{i,j}(i-m_x)^2\, x[i,j], \quad m_{yy} = \frac{1}{m}\sum_{i,j}(j-m_y)^2\, x[i,j], \tag{3.3}$$

$$m_{xy} = \frac{1}{m}\sum_{i,j}(i-m_x)(j-m_y)\, x[i,j], \tag{3.4}$$

with $m = \sum_{i,j} x[i,j]$. A translation of the image will influence m_x and m_y, where as rotation around the center (m_x, m_y) will influence m_{xx}, m_{xy}, m_{yy}. Shifting the image by $(-m_x, -m_y)$ and rotating it by $\alpha = \arctan(v_y/v_x)$ where v is the first eigenvector of the 2×2 matrix $M = [m_{xx}, m_{xy}; m_{xy}, m_{yy}]$ will create an image in normalized form with $m_x = m_y = m_{xy} = 0$ and $m_{xx} = m_{yy} = 1$, see Figure 3.3(b).

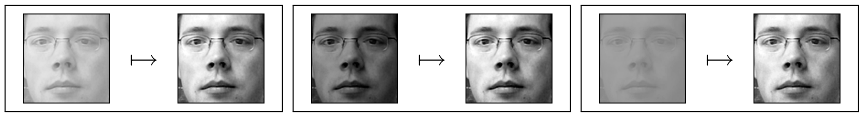

(a) *Illumination invariance* by brightness and contrast normalization. The right images are derived from the left by linearly transforming the grayvalues such that their minimum is 0 and their maximum is 1.

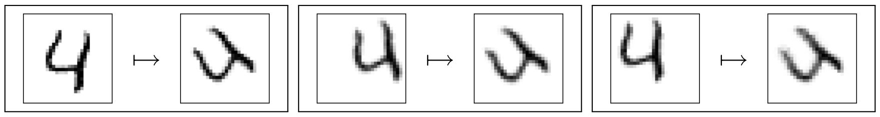

(b) *Geometric invariance* by moment normalization. The right images is derived from the left ones by translation and rotation such that $m_x = m_y = m_{xy} = 0$ and $m_{xx} = m_{yy} = 1$.

Figure 3.3 Invariance through *image normalization*: transforming the image to a *standard representation* can remove the effect of image variability.

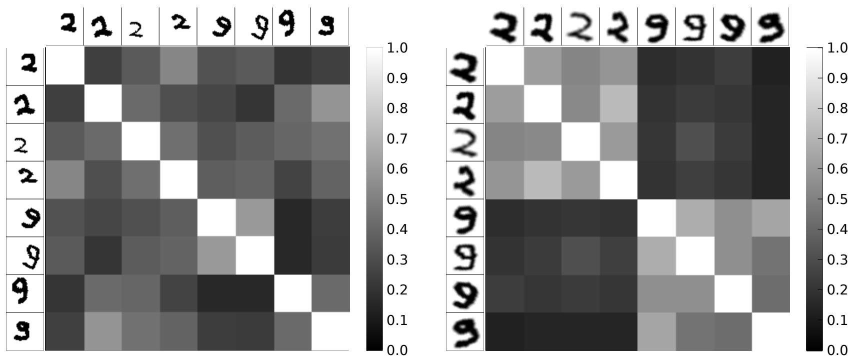

Figure 3.4 Effect of normalization on Gaussian kernel matrix: raw input samples (left) can have large Euclidean distance even if they belong to the same class. This leads to a non-informative kernel. Normalizing each sample to uniform size, translation and rotation (right) makes images of the same class more similar to each other, causing a more informative kernel matrix.

Advantages: Normalized images show fewer unwanted variations. Visually similar images become more similar also when treated as vectors. Thus, ordinary kernels for vector representations can be applied.

Disadvantages: An *inverse map* is required that counteracts the possible image distortions. Estimating the parameters of the normalization procedure for each image can be unreliable.

Conclusion: Use *image normalization* if you know how to define a *reference* configuration and how to reliably transform the images to it.

3.2.3 Invariant Kernel Functions

Instead of estimating normalizing parameters for each image and calculating the kernel values afterwards, one can make the normalization a part of the kernel function itself. This has the advantage that no globally best reference frame is required, but only transformations suitable to compute the distance between pairs of samples have to be estimated at a time. For example, instead of calculating the Gaussian kernel based on the Euclidean distance $\|.\|$, we define a new (dis)similarity measure based on finding the best match between the sample x and all distorted versions of x':

$$d_{match}(x, x') = \min_{J \in \mathcal{J}} \|x - J(x')\|^2 \tag{3.5}$$

where J runs over all distortion operators from a set $\mathcal{J}$, *e.g.* all rotations or translations. $\mathcal{J}$ is typically multidimensional and a full non-linear optimization over all elements is often too time consuming. Therefore, linear approximations have been developed, *e.g.* the *tangent distance* [Simard et al., 1999]:

$$d_{TD}(x, x') = \min_{\delta_1, \dots, \delta_k \in \mathbb{R}} \|x - (x' + \delta_k t_k)\|^2 \tag{3.6}$$

where t_k are the difference vectors between x' and a slightly distorted versions of x', *e.g.* the image shifted by 1 pixel horizontally or vertically, or rotated by a few degrees. From the (symmetrized) distance functions d_{match} or d_{TD} one can form invariant kernel functions:

$$k_{inv}(x, x') = e^{-\gamma [d(x,x') + d(x',x)]}. \tag{3.7}$$

An alternatively way of making the kernel values invariant to known image distortions is by averaging or integrating over the set of all possible transformations. We define

$$k_{int}(x, x') = \int_{J \in \mathcal{J}} \int_{J' \in \mathcal{J}} k(\, J(x), J'(x')\,) \tag{3.8}$$

for any image kernel k. If the set of transformation $\mathcal{J}$ is suitable, *e.g.* if it is a compact group [Haasdonk and Burkhardt, 2007], the resulting kernel function k_{int} will be exactly invariant to any of the transformations contained, even if k was not.

Advantages: By pairwise normalization, we can achieve invariance even if no global reference frame is available. By integrating over all of transformations, complete invariance can be achieved.

Disadvantages: Each kernel evaluation becomes slower to calculate. Distances functions that include optimization procedures can lead to kernel functions that are not positive definite.

Conclusion: Use an *invariant kernel* if image normalization as a preprocessing step is not possible, and if the transformation space is small enough such that efficient search or integration over it is feasible.

3.2.4 Invariant Representations

As we have seen in the *Introduction*, using a kernel function $k : \mathcal{X}\times\mathcal{X} \to \mathbb{R}$ is equivalent to choosing an implicit feature map $\varphi : \mathcal{X} \to \mathcal{H}$, where $\mathcal{X}$ is the set of all images and $\mathcal{H}$ is the Hilbert space induced by k. For invariant kernels, the induced feature map is insensitive to image variations, whereas in image normalization, we used an explicit preprocessing step $\mathcal{N} : \mathcal{X} \to \mathcal{X}$ that removed the influence of the unwanted variations from all images before applying φ. We can generalize both concepts by extracting *invariant features*, followed by an arbitrary kernel for the resulting representation. Mathematically, each of these operations corresponds to an explicit feature mapping $\psi : \mathcal{X} \to \tilde{\mathcal{X}}$, which is followed by the implicit mapping $\varphi : \tilde{\mathcal{X}} \to \mathcal{H}$ induced by a kernel function $k : \tilde{\mathcal{X}} \times \tilde{\mathcal{X}} \to \mathbb{R}$.

Because invariant feature maps form the basis for many relevant computer vision kernels, we will study some typical examples in the rest of this chapter. We will concentrate on achieving invariance to *changes in image appearance* without explicit distinction whether these are due to changes in the camera viewpoint, due to changes in the pose or shape of an objects, or due to inherent intra-class variance, as it is the case when comparing different object from a common object category.

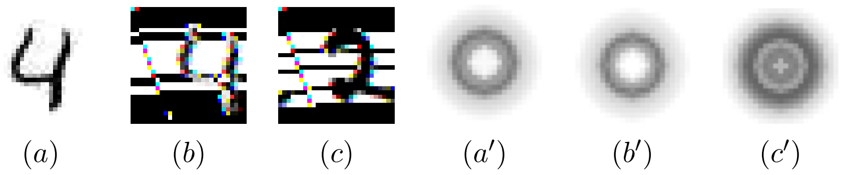

Figure 3.5 Rotation invariant features by integration. (a),(b): The two digits 4 differ by a rotation, which makes them dissimilar them in a Euclidean sense. (a'),(b'): Averaging over all their rotated versions yields very similar images. (c),(c'): The average over all rotated versions of a digit 2 image yields a feature image clearly different from (a') and (b').

While this point of view is predominant in current computer vision research, one should note that there is also a large amount of classical work studying specific aspects of geometric invariance, see *e.g.* [Mundy and Zisserman, 1992] and [Wood, 1996] for overviews.

Advantages: *Invariant feature mapping* allow the efficient removal of many sources of unwanted image variations, even if no normalization procedure is known.

Disadvantages: By choosing a too uninformative intermediate representation, important sources of variance are easily removed as well. Because the feature extraction is always applied first, there is no way to recover the lost information.

Conclusion: *Invariant feature mappings* form the basis for most relevant computer vision kernels. However, one has to take care in their design to remove only the right amount of variations.

3.2.4.1 Integration-Based Invariant Features

Already linear or almost-linear transformations, *e.g.* integration against a weight function or the taking of absolute values, can make images more *invariant*. A special role is taken by the Fourier transform $\mathcal{F}$: a common way to achieve translation invariance in signals is by calculating the absolute values in the Fourier domain $|\mathcal{F}x|$.

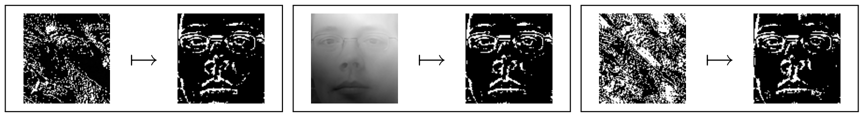

Figure 3.6 Edge detection as invariant preprocessing step: image differentiation followed by thresholding removes global intensity variations while keeping the location of edges.

A similar effect as computing the invariant kernel (3.8) can be achieved by extracting features from Haar-integrals, *e.g.* the radial profile after integrating over all rotated version of an image $\tilde{x} = \int_{\theta\in[0,2\pi]} R_\theta(x)\, d\theta$, where $R_\theta x$ denotes the result of rotating the image x by an angle of θ. See Figure 3.2.4.1 for an illustration.

3.2.4.2 Edge-Based Invariant Features

In natural images, the location and orientation of edges is often more important than absolute intensity values. This has led to a variety of edge-based feature maps, typically obtained by applying a differentiation filter to the image, *e.g.* the *Sobel* or *Laplace* operator, and thresholding the response. Figure 3.6 illustrates this operation. Because differentiation is specifically susceptible to noise, it is often helpful to first convolve the input images with a Gaussian filter in order to *denoise* them. The result is a *Gaussian derivative filter*, which in a similar form is known to also exist in the human visual system [Young, 1987].

3.2.4.3 Histograms-Based Invariant Features

A lot of unwanted variance in natural images is due to changes in the viewpoint, as is illustrated in Figure 3.7. Compared to the in-plane rotations of Figure 3.2.4.1, such variations are much more difficult to parameterize and remove, because in perspective projections information is lost that cannot be recovered by a mere postprocessing operation. Therefore, we cannot hope to define a normalizing transformations that exactly removes the visual effects of changes in perspective. However, we can define feature maps that are largely invariant to perspective effects (or other geometric image properties) using *feature counts* that are aggregated into *histograms*: for a selection of localized base features

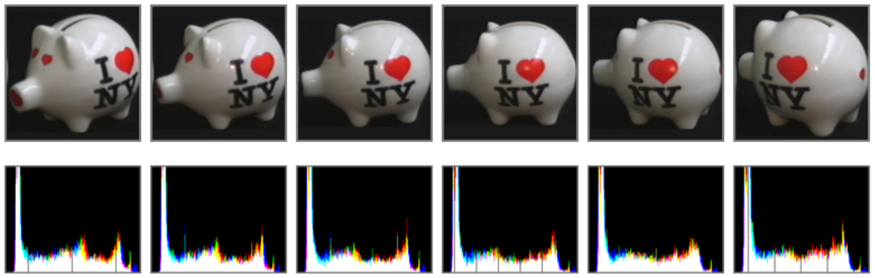

Figure 3.7 Color histograms as perspective invariant features: the same object results in different images when viewed from different viewpoints. Nearly the same parts occur, but in different locations. The images differ when treated as vectors, but their color histograms are almost identical. Images: Colorado Object Image Library [Nene et al., 1996]

one counts how frequently each possible value occurs in the image, irrespective of its position. For practical reasons, low-dimensional quantities are preferable as base features. By quantizing their value range into a fixed number of bins, the resulting histograms have fixed length and can be treated like vectors.

The amount of invariance achieved by this construction depends on the base feature used. For geometrically insensitive quantities such as the *grayscale value* or the *color* of a pixel, the resulting histogram will be invariant to most geometric transformations, in particular translations and rotations. Oriented base features, such as the *gradient direction* at each pixel will result in representations that are insensitive to translations, but still sensitive to rotations.

Because feature count histograms discard the global geometry in the image and keep only what is measured locally by the base features, they also provide invariance against many non-rigid geometric image distortions, and limited amount of out-of-plane rotations, see Figure 3.7. Of course, all image based measures fail to detect similarity on a purely semantic level, *e.g.* between the front side and the back side of an object, if these do not look similar.

Histogram representations can discard all geometric information from an image, even potentially relevant one. A way to control up to what scale the geometric information is removed is provided by *local-*

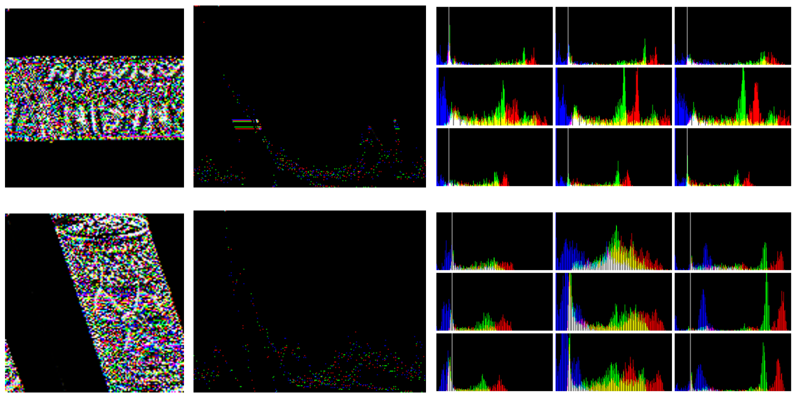

Figure 3.8 Color histograms ignore all geometric relations, therefore very different objects (left) can have similar histogram representations (middle). By forming histograms over smaller image regions, *e.g.* the cells of a 3×3 grid (right), the feature map can be made more specific. On a global level it retains geometry but locally it is still invariant to changes *e.g.* due to perspective. Images: Colorado Object Image Library [Nene et al., 1996]

ized histograms [Smith and Chang, 1996], as illustrated in Figure 3.8. Instead of a single histogram per image, several histograms over predefined regions are formed, typically over one or several rectangular grids. By concatenating the resulting histograms, one again obtains a single feature vector. Depending on the size and number of regions chosen, it will be more or less invariant to geometric variations of the image.

3.3 Region-Based Image Representations

Advanced computer vision tasks require generalization not only between different views of the same objects, but between many different objects that only share a semantic aspect, *e.g.* animals of the same species. The visual variations within such a class can be very large, see *e.g.* Figure 3.9. An additional complication arises from the fact that the objects of interest often cover only a small parts of the image and that they can be truncated or occluded. *Region-based* representations of natural images have been developed to overcome all of these problems. They are based on the idea of treating the image as collections

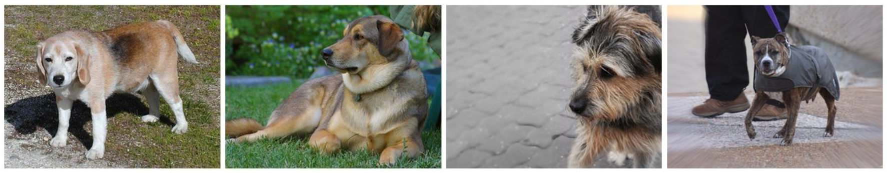

Figure 3.9 Object of the same semantic category, here *dog*, can differ greatly in appearance because of intra-class variance, change of pose, truncation, or occlusion. However, typical characteristic parts are often common for all object instances, *e.g.* eyes, ears or legs, thereby distinguishing them from other categories. *Images courtesy of photos8.com, pdphoto.org.*

of many local regions instead of as single object with global properties. First approaches in this direction concentrated on models with very few *parts* that had a semantic meaning, *e.g.* the *eyes* and *mouth* in a face [Fischler and Elschlager, 1973], or the *wheels* of a vehicle [Fergus et al., 2003]. More recently, statistical approaches have become dominant that can make use of thousands of image regions, many of which represent low-level appearance properties of the image, *e.g.* corners or edges [Lowe, 2004].

3.3.1 Interest Points and Descriptors

To identify relevant regions in the image, one first applies an operator for the detection of *interest points*. Typically, these are low-level differential filters based on *differences of Gaussian* [Harris and Stephens, 1988; Lowe, 2004; Mikolajczyk and Schmid, 2004] or Wavelet coefficients [Loupias et al., 2000; Bay et al., 2006] that at the same time allow the extraction of a characteristic scale to form *regions of interest*. Alternatively, interest points on a regular grid [Deselaers et al., 2005] or random locations and scales [Nowak et al., 2006] can also work well in practice.

Each region of interest defines a small image from which one calculates an *invariant representation*, often called a *descriptor*. The popular SIFT descriptor [Lowe, 2004] does this by combining several ideas of the previous sections: it normalizes the image region with respect to size and a canonical orientation, it smoothes the image to remove noise, it calculates image gradients for increased illumination invariance, and it aggregates the gradient directions into localized histograms for a certain degree of geometric invariance. Many other descriptors have been developed that follow similar design goals. A recent survey can be found *e.g.* in [Tuytelaars and Mikolajczyk, 2008].

After this first preprocessing step, the image is represented as a set of descriptor vectors, one per region of interest in the image. All descriptors vectors are of the same length, typically between 20 and 500 dimensions. The number of regions and descriptors varies depending on the image contents and on the method for interest point detection, typically between 100 to 50,000.

3.3.2 Set Kernels for Region-Based Representations

In order to define kernels between images in region-based representations, one has to overcome the problem that images are represented by different numbers of regions of different size at different locations. As simplest solution one ignores all geometric properties of the regions of interest, and one keeps only the vector valued descriptors [Wallraven et al., 2003]. This leaves one with the problem of comparing two images, $x = \{d_1, \dots, d_m\}$ and $x' = \{d'_1, \dots, d'_{m'}\}$, that are represented by sets of possibly different numbers of descriptor vectors.

Analogously to Equations (3.7) and (3.8), there are two canonical ways to define the similarity between such sets of vectors, either by *summing* over all values of vector-level base kernels, or by finding the best *match* for each element:

$$k_{sum}(x, x') := \sum_{i=1}^{m} \sum_{j=1}^{m'} k(d_i, d'_j) \tag{3.9}$$

and

$$k_{match}(x, x') := \frac{1}{m} \sum_{i=1}^{m} \max_{j=1,\dots,m'} k(d_i, d'_j) + \frac{1}{m'} \sum_{j=1}^{m'} \max_{i=1,\dots,m} k(d_i, d'_j), \tag{3.10}$$

where k is any base kernel between vectors.

Unfortunately, such *set kernels* are often computationally inefficient, because the computational effort for each kernel evaluation is quadratic in the number of descriptors per image.

3.3.3 Pyramid Match Kernel

The quadratic complexity of comparing two images in region based representation can be reduced to linear complexity by quantizing the space of possible descriptor values. The *pyramid match kernel (PMK)* [Grauman and Darrell, 2005] does so by subdividing the d-dimensional space of image descriptors into a hierarchy of axis parallel cells in a data dependent way. In the finest layer, each descriptor lies in a cell of its own. Coarser layers are built by merging neighboring cells in any dimension. Consequently, every new cell consists of 2^d cells of the previous layer and this construction is repeated until the coarsest layer has only one cell containing all descriptors.

The base kernel $k(d_i, d'_j)$ of the matching kernel (3.10) is approximated by a count in how many cells both descriptors lie together. This yields a final kernel definition of

$$k_{PMK}(x, x') = \sum_{l=1}^{L} 2^l \sum_{k=1}^{2^{l-1}} \min\left(h^{l,k}(x), h^{l,k}(x')\right), \tag{3.11}$$

where $h^{l,k}(x)$ are histograms of how many features of the image x fall into the k-th cell of the l-th pyramid level. By pre-computing these and storing only the non-empty bins, each evaluation of k_{PMK} requires $O(\max(m, m')dL)$ operations, where L is the number of pyramid levels. Since the number of descriptors per image is typically large, whereas L is small, this is much faster than the $O(mm'd)$ complexity of the naïve matching kernel.

3.3.4 Feature Codebooks

Natural images have inherent regularities that cause the extracted descriptors vectors to form *clusters* in the descriptors space. For example, edges and corners are typically much more frequent than checker board-like patterns. A quantization of the descriptor space by a regular grid, as used by the pyramid match kernel, does not reflect this clustering: on the one hand, a large number of grid cells will stay empty, and on the other hand, existing clusters might be split apart, see Figure 3.10. A way to overcome this problem is by identifying a relatively small

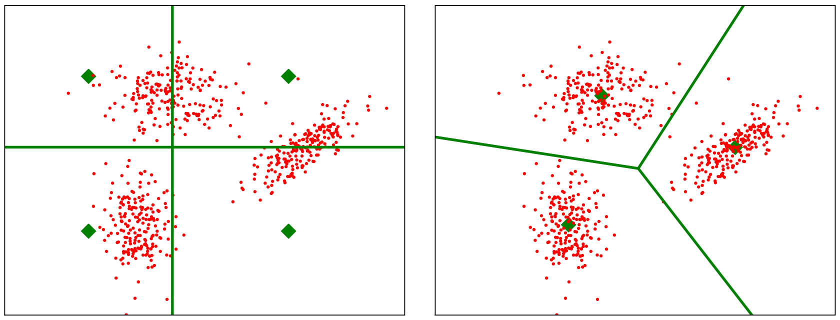

Figure 3.10 Descriptor Codebooks: The descriptors that occur in natural images do not lie uniform in the space of all possible descriptors, but they form clusters. Axis-parallel subdivisions (left) do not respect the cluster structure and can cut through regions of high density. Clustering the descriptors followed by vector quantization (right) divides the descriptor space into Voronoy cells that respect the cluster structure.

number of cluster centers in the descriptor space and quantizing the feature space by the induced Voronoy tessellation. Cluster centers are usually determined by a K-means clustering of all descriptors in the training data, or a subset thereof. Subsequently, for each descriptor set d_i in an image x, the nearest cluster center c_k (also called *codebook vector* or *visual word*) is identified. As simplest representation, we count for each cluster center how often it occurs as a nearest neighbor of a descriptor in x and form the resulting K-bin histogram [Sivic and Zisserman, 2003]. This construction is often called *bag of visual words*, since it is similar to the *bag of words* concept in *natural language processing*. The term *bag* indicates that all (quantized) descriptors are put into a single, unordered, representation, irrespectively of their original local or global arrangement in the image.

3.3.5 Kernels for Bag of Visual Words Representations

The representation of images as feature count histograms leaves us with many possibilities which kernel function to apply to them. A direct analogue of the pyramid match kernel (3.11) is the *histogram intersection*[2]

[2] This measure of similarity between histogram representations of images has been popularized earlier by [Swain and Ballard, 1991]. However, it was proved only much later that

kernel:

$$k_{HI}(x,x') = \sum_{k=1}^{K} \min(h^k, h'^k), \tag{3.12}$$

where we write $h = (h^1, \dots, h^K)$ for the K-bin histogram representation of x and analogously h' for the histogram of x'.

For fixed length histograms we can apply all kernels defined for vectors, *e.g. linear*, *polynomial* or *Gaussian* [Csurka et al., 2004]. If the number of feature points differs between images, it often makes sense to first normalize the histograms, *e.g.* by dividing each histogram bin by the total number of feature points[3]. This allows the use of kernels for empirical probability distributions, *e.g.* the *Bhattacharyya kernel*

$$k_{bhattacharyya}(x,x') = \sum_{k=1}^{K} \sqrt{h^k h'^k} \tag{3.13}$$

or the *symmetrized KL-divergence kernel*

$$k_{symKL}(x,x') = \exp\left(-\frac{1}{2}(KL(h|h') + KL(h'|h))\right), \tag{3.14}$$

where $KL(h|h') = \sum_k h^k \log \frac{h^k}{h'^k}$. A particularly popular choice in computer vision is the χ^2*-kernel*:

$$k_{\chi^2}(x,x') = \exp\left(-\gamma \sum_{k=1}^{K} \frac{(h^k - h'^k)^2}{h^k + h'^k}\right), \tag{3.15}$$

that can be seen as an approximation to k_{symKL} with better numerical properties and that has shown very good performance, *e.g.* in object classification tasks [Zhang et al., 2007].

k_{HI} is in fact a positive definite kernel function, see Odone et al. [2005].

[3] Which normalization procedure is the *best* for bag of visual word histograms is as disputed as the question which kernel function to use. Apart from normalization the histograms by their L^1 or L^2 norm, it has been proposed, *e.g.* take square or cubic roots of entries [Jiang et al., 2007] or to *binarize* at a fixed or adaptive threshold [Nowak et al., 2006]. Alternatively, per-bin weighting schemes, such as *bi-normal separation* [Forman, 2003] or *tf-idf* [Hiemstra, 2000], that originated in text processing have also been applied to visual word histograms.

3.3.6 Spatial Pyramid Representations

The *bag of visual words* representation discards all information about spatial structure from the image, as we have seen previously for other histogram representations. However, spatial information can be a valuable source of information, *e.g.* in image segmentation, where *sky* regions tend to occur much more frequently at the top of the image than at the bottom. Consequently, the idea of *local histograms* has been adapted to this context as well. Instead of one global visual word histogram, a number of local histograms are formed, typically in a pyramid structure from coarse to fine. Each subhistogram has K bins that count how many descriptors with center point in the corresponding pyramid cell have a specific codebook vector as nearest neighbor. Subsequently, either all local histograms are concatenated into a single larger histogram [Lazebnik et al., 2006], or separate kernel functions are applied for each level and cell, and the resulting kernel values combined into a single *spatial pyramid* score, *e.g.* by a weighted sum [Bosch et al., 2007]:

$$k_{SP}(x, x') = \sum_{l=1}^{L} \beta_l \sum_{k=1}^{K_l} k\left(h_{(l,k)}, h'_{(l,k)}\right), \tag{3.16}$$

where L is the number of levels and β_l is a per-level weight factor. K_l is the number of cells in the l-th level, and $h_{(l,k)}$ and $h'_{(l,k)}$ are the local histograms of x and x' respectively. The base kernel k is typically chosen from the same selection of histogram kernels as above, with or without prior histogram normalization.

4

Classification

Classification with support vector machines (SVMs) is the most popular application of kernel methods in computer vision. However, in contrast to the discussion in the *Introduction*, realistic classification problems are often not just binary decisions but involve multiple possible class labels. In the following, we discuss extensions of SVMs that are capable of working with multiclass data. Subsequently, we give examples from the recent computer vision literature where kernel classifiers have successfully been applied to tasks like *object classification*, *scene classification* and *action classification*.

4.1 Multiclass Support Vector Machines

The hyperplane based classifiers that form the basis of SVMs are only suitable for binary decision problems. To overcome this limitation, several variants of SVMs have been developed that can handle more than two output classes by decomposing the multiclass decision step into a collection of binary decisions.

4.1.1 One-versus-rest Multiclass SVM

The simplest form of multiclass classification with SVMs is the *one-versus-rest* formulation [Vapnik, 1998]. For a classification problem with M classes, we train M support vector machines $f_1, \dots, f_M$, each using the examples of one class as positive training examples and the examples of all other classes as negative training examples. To classify a test example, all SVMs are evaluated, and the class label of the SVM with largest value of the decision functions is selected:

$$F(x) = \operatorname*{argmax}_{m=1,\dots,M} f_m(x). \tag{4.1}$$

One-versus-rest multiclass SVMs achieve good classification performance [Rifkin and Klautau, 2004], and they are very popular in computer vision because their simple setup makes them easy to implement and evaluate.

4.1.2 One-versus-one Multiclass SVM

When the number of classes is large, the binary problems that one-versus-rest SVMs have to solve become very unbalanced. An alternative setup that avoids this problem are *one-versus-one* multiclass SVMs [Hsu and Lin, 2002]. Their underlying idea is to train one SVM per pair of class labels, $f_{i,j}$ for $1 \leq i < j \leq M$, always using the samples of one class as positive and the samples of the other class as negative training examples. To classify a test sample, all SVMs are evaluated, and a voting is performed, which class label was selected most often.

$$F(x) = \operatorname*{argmax}_{m=1,\dots,M} \#\{i \in \{1, \dots, M\} : f_{m,i}(x) > 0\}, \tag{4.2}$$

where for convenience we used the notation $f_{j,i} = -f_{i,j}$ for $j > i$ and $f_{j,j} = 0$. If the argmax is not unique, *i.e.* there are several classes having the same maximal number of positive SVM decisions, some form of tie breaking is required. Typically one just selects one of the majority classes at random. Although the one-vs-one setup requires many more SVMs to be trained and evaluated, each is based on a smaller training set, thus making the one-vs-one multiclass SVM approximately equally fast as the one-vs-rest multiclass SVM.

4.1.3 Crammer-Singer Multiclass SVM

While the one-vs-rest and one-vs-one SVMs consist of several independently trained binary classifiers, the multiclass SVM proposed by [Crammer and Singer, 2001] uses a training procedure that find solution hyperplanes $w_1, \dots, w_M$ for all classes from a joint optimization formulation:

$$\min_{\substack{w_1,\dots,w_M \in \mathcal{H} \\ \xi_1,\dots,\xi_n \in \mathbb{R}^+}} \sum_{m=1}^{M} \|w_m\|^2 + \frac{C}{n} \sum_{i=1}^{n} \xi_i \tag{4.3}$$

subject to

$$\langle w_{y_i}, \varphi(x_i)\rangle - \langle w_{y'}, \varphi(x_i)\rangle \geq 1 - \xi_i, \qquad \text{for } y' \neq y_i \tag{4.4}$$

for $i = 1, \dots, n$. The classification function

$$F(x) = \operatorname*{argmax}_{m=1,\dots,M} f_m(x) \tag{4.5}$$

with $f(x) = \langle w, \varphi(x_i)\rangle_{\mathcal{H}}$ is of the same form as in the one-vs-rest situation.

Analyzing the optimization problem shows that the Crammer-Singer SVM training differs from the training of M independent SVMs in the one-vs-rest setup only in the constraints (4.4). Ordinary SVM training enforces $y_i f(x_i) \geq 1 - \xi_i$, *i.e.* each sample x_i should lie on the right side of the decision hyperplane and have a margin of at least 1 from the wrong side. The Crammer-Singer SVM enforces $f_m(x_i) - f_{m'}(x_i) \geq 1 - \xi_i$ for each $m' \neq m$, *i.e.* each training sample should be classified correctly under the decision rule (4.5), and have a margin of at least 1 from being classified as any of the other (and thereby wrong) classes. One can check that for $M = 2$, the optimization problem will yield $w_1 = -w_2$, which reduces the Crammer-Singer SVM to an ordinary binary SVM.

4.1.4 Other Multiclass SVM

Several other multiclass SVM variants have been developed for special situations: [Platt et al., 1999] build a *directed acyclic graph (DAG)* out of the $M(M-1)/2$ binary SVMs of the *one-versus-one* setup. By traversing along the DAG, only $(M-1)$ SVM evaluations are required to come to a prediction, thus speeding up the multiclass decision (4.2).

In order to make the decision process more robust, multiclass SVMs based on *error-correcting codes* have been developed [Dietterich and Bakiri, 1995]. They introduce a certain redundancy into the decomposition of the multiclass decision problem into several binary decisions, By arranging the binary decisions in an *error-correcting code*, robustness to mistakes in the outcome of any of the binary decisions is achieved.

Overall, none of the multiclass SVM formulations has proven clearly superior to the others in terms of classification accuracy. It depends on the problem at hand, which training and test setup is most appropriate.

4.2 Example: Optical Character Recognition

B. Schölkopf, C. Burges, and V. Vapnik: *"Extracting Support Data for a Given Task"*, Knowledge Discovery and Data Mining, 1995.

In one of the earliest application of a kernel-based classifier to a computer vision problem, [Schölkopf et al., 1995] use a support vector machine with polynomial, Gaussian or sigmoid kernel to classify handwritten digits in a a one-versus-rest setup. Apart from reporting improved error-rates, the authors show that the number of support vectors is only 4% of the dataset, making the evaluation procedure more efficient that, for example, a nearest neighbor classifier.

4.3 Example: Object Classification

G. Csurka, C. R. Dance, L. Fan, J. Willamowski and C. Bray: *"Visual categorization with bags of keypoints"*, ECCV Workshop on Statistical Learning in Computer Vision 2004.

In order to perform object classification in natural images, [Csurka et al., 2004] introduce the *bag of visual words* representation. As a proof of concept, they train a one-versus-rest support vector machine with linear kernel and achieve higher classification accuracy than a Naïve-Bayes classifier on a seven class natural image dataset.

K. Grauman and T. Darrell: *"The Pyramid Match Kernel: Discriminative Classification with Sets of Image Features"*, ICCV 2005.

In this work [Grauman and Darrell, 2005] introduce the *pyramid match kernel* (3.11) for comparing two images that are represented by different numbers of local feature descriptors. The kernel is used in a one-versus-rest multiclass support vector machine for object classification on the ETH80 and Caltech101 datasets. Compared to the *matching* kernel (3.10), the pyramid match kernel is shown to be faster to compute and to achieve higher classification accuracy.

4.4 Example: Scene Classification

S. Lazebnik, C. Schmid, and J. Ponce: *"Beyond Bags of Features: Spatial Pyramid Matching for Recognizing Natural Scene Categories"*, TR 2005

The authors introduce the *Spatial Pyramid Matching* (3.16) kernel, based on a representation of images as a pyramids of increasingly localized bag of visual word histograms [Lazebnik et al., 2006]. The histograms of each pyramid level and cell are compared by the histogram intersection kernel (3.12) and combined into an overall kernel value by a weighted linear combination. In combination with a one-versus-rest multiclass SVM, the kernel is shown to outperform kernels flat bag of visual word kernels.

4.5 Examples: Action Classification

P. Dollár, V. Rabaud, G. Cottrell, and S. Belongie: *"Behavior Recognition via Sparse Spatio-Temporal Features"*, CVPR 2006

[Dollar et al., 2005] generalize the bag-of-visual-word concept to *spatio-temporal words* that allow a sparse representation of video sequences. In a one-versus-rest SVM with Gaussian kernel, this representation achieved better classification performance than a 1-nearest neighbor classifier for the classification of *facial expressions* and *human activities*. Interestingly, [Nowozin et al., 2007] later achieved even higher classification performance when repeating the experiments with identical feature representation but using extensive cross-validation to determine the SVM parameters. This shows that, even though SVMs are relatively robust against changes of their parameters, model selection should not be neglected as part of the training procedure in order to achieve the highest possible accuracy.

5

Outlier Detection

Data intensive computer vision tasks, such as image retrieval or video surveillance, typically work with many thousand images, but not always do they have access to reliable class labels in order to train a classifier. *Outlier* or *anomaly detection* are frequently applied techniques in this situation: outlier detection helps to "clean" a dataset by removing examples that are too different from all other samples. A typical example would be mislabeled examples returned by a search query. In anomaly detection, it is the non-typical samples that are the main objects of interest. This is a common preprocessing step, *e.g.* in surveillance tasks, where no new information is gained by processing scenes that are very similar to already previously seen ones. Methodically, both methods are basically identical, as they have the goal of identifying data points that are different from most other ones. In the following, we introduce two related techniques that are applicable to both tasks: *support vector data description (SVDD)* and the *one-class support vector machine (OC-SVM)*.

5.1 Geometric Outlier Detection in $\mathbb{R}^d$

An intuitive way for outlier or anomaly detection consists of estimating the density of data points in the feature space. Samples in regions of high density are *typical*, whereas samples in low-density regions are not. However, density estimation in high-dimensional spaces is a notoriously difficult problem[1]. Instead, we adopt a more *geometric* approach: we model the high density region by only a single sphere with unknown location and size. Outlier detection then becomes the problem of finding the center $c \in \mathbb{R}^d$ and radius $R \in \mathbb{R}^+$ of the sphere such that most sample points $x_1, \ldots, x_n$ lie inside the sphere, *i.e.* they fulfill $\|x_i - c\| \leq R$. This task is formalized by the following optimization problem:

$$\min_{\substack{R\in\mathbb{R}, c\in\mathbb{R}^d \\ \xi_1,\ldots,\xi_n\in\mathbb{R}^+}} R^2 + \frac{1}{\nu n}\sum_{i=1}^{n} \xi_i \tag{5.1}$$

subject to

$$\|x_i - c\|^2 \leq R^2 + \xi_i \quad \text{for } i = 1, \ldots, n. \tag{5.2}$$

As in the case of support vector machines, we use slack variables ξ_i to allow some points, namely the outliers, to lie outside of the sphere, but they are penalized linearly in the objective function[2]. A parameter $\nu \in (0, 1]$ controls how many outliers are possible: the smaller ν the fewer points will be outliers, since violating the constraint (5.2) will be penalized more heavily. A more detailed analysis shows that νn is in fact a lower bound on number of outliers over the training set [Schölkopf and Smola, 2002].

Once we have learned the center point and the radius, we decide for new samples based on their distance to the sphere's center: if their

[1] This makes kernel-based outlier detection a classical instance of *Vapnik's principle*: *"If you possess a restricted amount of information for solving some problem, try to solve the problem directly and never solve a more general problem as an intermediate step [...]"* [Vapnik, 1998]

[2] For computational reasons, we rely on the same linear penalization of slack variables as in binary classification. One could argue that this is somewhat less intuitive here, because outliers are not "mistakes" in the one-class setup. However, solving the minimum enclosing sphere problem in a way such that outliers are completely ignored is in general NP-hard [Charikar et al., 2001], even if efficient approximation algorithms have been developed in *computational geometry* and *robust statistics*, see *e.g.* [Bădoiu et al., 2002].

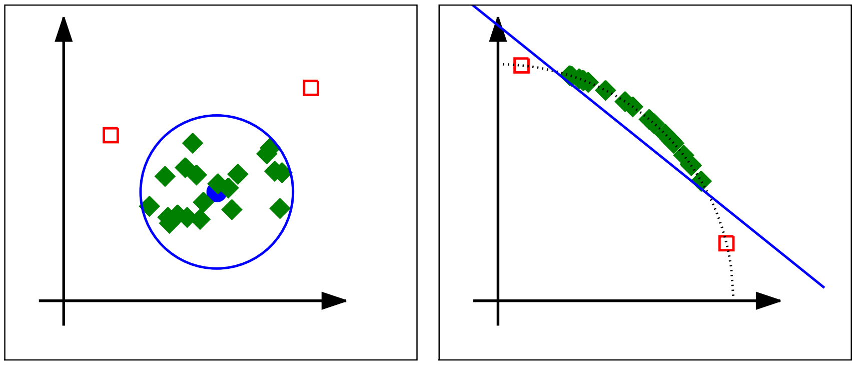

(a) Minimal enclosing sphere (b) Separating hyperplane

Figure 5.1 Outlier Detection: *support vector data description* (left) finds the smallest sphere that contains all samples (◆) except for some outliers (□). The *one-class SVM* (right) separates inliers (◆) from outliers (□) by finding a hyperplane of maximal distance from the origin. Both approaches are equivalent if all samples lie at the same distance from the origin and are linearly separable from it.

distance to the center is larger an R, they are considered outliers or anomalies, otherwise they are considered regular samples. A suitable decision function is given by

$$f(x) = R^2 - \|x - c\|^2. \tag{5.3}$$

where we have squared the individual terms to make f differentiable.

5.2 Support Vector Data Description

Support Vector Data Description (SVDD) [Tax and Duin, 2004] performs outlier detection in a latent feature space by kernelizing Equations (5.1) and (5.2). For a given kernel $k : \mathcal{X} \times \mathcal{X} \to \mathbb{R}$ with induced Hilbert space $\mathcal{H}$ and feature map $\varphi : \mathcal{X} \to \mathcal{H}$, the problem becomes

$$\min_{\substack{R\in\mathbb{R}, c\in\mathcal{H} \\ \xi_1,\dots,\xi_n\in\mathbb{R}^+}} R^2 + \frac{1}{\nu n}\sum_{i=1}^{n} \xi_i \tag{5.4}$$

subject to

$$\|\varphi(x_i) - c\|^2_{\mathcal{H}} \leq R^2 + \xi_i \quad \text{for } i = 1, \dots, n. \tag{5.5}$$

This is a *convex* optimization problem and can be solved efficiently even for several thousand data points. By use of the *Representer Theorem*, one obtains that the sphere's center point can be expressed as a linear combination $c = \sum_i \alpha_i \varphi(x_i)$ of the transformed data points. This allows us to evaluate the decision function only using kernel values:

$$\begin{aligned} f(x) &= R^2 - \|\varphi(x) - c\|^2_{\mathcal{H}} \\ &= R^2 - k(x,x) + 2\sum_{i=1}^{n} \alpha_i k(x_i, x) - \sum_{i,j=1}^{n} \alpha_i \alpha_j k(x_i, x_j) \end{aligned} \tag{5.6}$$

where the last sum is independent of x and can be merged with the constant R^2.

5.3 One-Class Support Vector Machines

A quick geometric check shows that if all data points have the same feature space norm and can be separated linearly from the origin, finding the minimal enclosing sphere is equivalent to finding a maximal margin hyperplane between the data points and the origin.

The *one-class support vector machine (OC-SVM)* [Schölkopf et al., 2001] relies on this linear construction, solving the corresponding optimization problem in the kernel-induced feature space:

$$\min_{\substack{R\in\mathbb{R}, w\in\mathcal{H} \\ \xi_1,\dots\xi_n\in\mathbb{R}^+}} \|w\|^2_{\mathcal{H}} + \frac{1}{\nu n}\sum_{i=1}^{n} \xi - \rho \tag{5.7}$$

subject to

$$\langle w, \varphi(x_i)\rangle_{\mathcal{H}} \geq R - \xi_i, \qquad \text{for } i = 1, \dots, n. \tag{5.8}$$

Since the problem is very similar to the support vector machine optimization, it can be solved efficient by optimization techniques originally developed for binary classification with SVMs. The resulting decision function

$$f(x) = \sum_{i=1}^{n} \alpha_i k(x_i, x) - R \tag{5.9}$$

is in fact identical to the decision function of an SVM (2.30) with bias term R. Note that many kernels in computer vision, *e.g.* Gaussian and

χ^2-kernel, have the properties that $k(x, x) = 1$ for all $x \in \mathcal{X}$. In this case, the underlying geometric problems of SVDD and OC-SVM are identical, and both methods learn the same decision functions.

5.4 Example: Steganalysis

S. Lyu and H. Farid: *Steganalysis Using Color Wavelet Statistics and One-Class Support Vector Machines*, Proceedings of SPIE, 2004

The task of steganalysis, *i.e.* the problem of detecting whether a given image contains a hidden signal, is close related to the problem of finding anomalies. [Lyu and Farid, 2004] train a one-class SVM with Gaussian kernel for this purpose using steganography-free images in a multi-scale multi-orientation wavelet representation as input. Afterwards, images that the OC-SVM classifies as outliers are considered potential carriers of a hidden steganographic signal. By the use of a one-class setup, the method is applicable for all steganographic processes, not only for those for which training data is available.

5.5 Example: Image Retrieval

Y. Chen, X. Zhou, and T. S. Huang: *"One-Class SVM for Learning in Image Retrieval"*, ICIP 2001

In order to perform image retrieval with user feedback, [Chen et al., 2001] train a one-class SVM with linear or Gaussian kernel on the images that the users marks as relevant. Subsequently, new images are ranked according to the output of the trained system. In contrast to the more common two-class setup, the authors argue that a one-class setup better reflects the user intend in image retrieval scenarios, because typically the relevant images have similar feature representations, whereas images that are not of interest to the user lie spread out over all of the feature space.

6

Regression

Regression problems emerge frequently in data analysis, and the mathematics underlying *linear regression* techniques is well-understood. However, for high-dimensional problems as they occur in computer vision the performance of linear regression methods is often not satisfactory. By *kernelizing* linear regression techniques, non-linear functions can be included into the model class, while still retaining the largest part of the theoretical background. This opens new possibilities for the use of regression methods also in computer vision applications, *e.g.* for *pose estimation* or in *image superresolution*.

In the following, we introduce *kernel ridge regression* and *support vector regression* as the most important kernel-based regression techniques, and we give examples of their successful application for state-of-the-art computer vision tasks[1].

[1] We do not include *Gaussian Process (GP) Regression* in our discussion, as its interpretation of the kernel is more as a covariance function than as the inner product in a high-dimensional feature space. See [Rasmussen and Williams, 2006] for an excellent introduction to Gaussian Processes.

6.1 Kernel Ridge Regression

Linear regression in its simplest form deals with the problem of predicting a linear function $f : \mathbb{R}^d \to \mathbb{R}$ from samples $x_i \in \mathbb{R}^d$ with corresponding target values $y_i \in \mathbb{R}$. Because f is assumed linear, it can be parameterized by a weight vector $w \in \mathbb{R}^d$ as

$$f(x) = \langle w, x \rangle + b, \tag{6.1}$$

showing that the problem is closely related to the problem of classification studied before. As for classification, we will simplify the notation by assuming that a component of constant value 1 has been appended to the vector x such that the bias term b can be absorbed into the weight vector w.

In contrast to classification, where we only need to learn a function f that fulfills $f(x_i) > 0$ for the samples of one class and $f(x_i) < 0$ for the others, in regression we need to solve the more difficult problem of achieving $f(x_i) \approx y_i$ for all training samples. Different methods for linear regression differ in how they penalize errors, *i.e.* points x_i for which $f(x_i) \neq y_i$. A classical choice is *least-squares regression* that determines the weight vector w by the following minimization problem:

$$\min_{w \in \mathbb{R}^d, b \in \mathbb{R}} \frac{1}{2} \sum_{i=1}^{n} (\langle w, x_i \rangle - y_i)^2 + \lambda \|w\|^2. \tag{6.2}$$

The first term penalizes deviations between $f(x_i)$ and y_i, called the *residua*, with quadratic cost. The second term is a regularizer that is optional, but typically improves prediction performance as it penalizes too large weights. Linear least-squares regression is particularly popular because Equation (6.2) has a closed form solution

$$w = X(\lambda I_n + X^T X)^{-1} y \tag{6.3}$$

where I_n is the n-dimensional identity matrix, $X = (x_1, \dots, x_n)^t$ is the matrix formed by the sample points and $y = (y_1, \dots, y_n)^t$ is the vector containing the target values.

Kernel ridge regression (KRR) [Saunders et al., 1998] is obtained by *kernelizing* Equation 6.2: for a given kernel function $k : \mathcal{X} \times \mathcal{X} \to \mathbb{R}$, we replace x_i by the induced $\varphi(x_i)$. The closed form solution formula is valid in this situation as well, and if we replace X by $\Phi =$

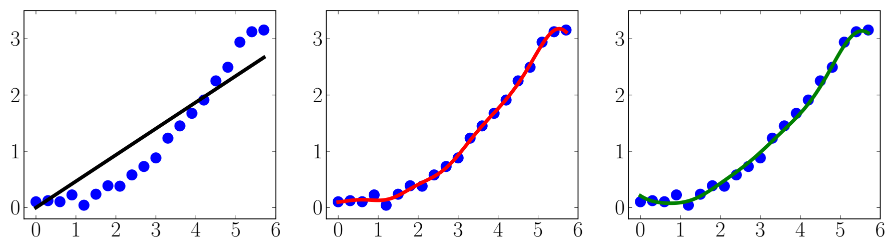

(a) regression without outliers

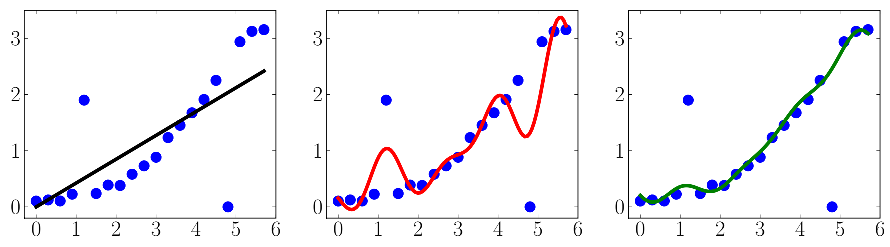

(b) regression with outliers

Figure 6.1 Linear regression (left) is not able to fit non-linear functions. kernel ridge regression (middle) can fit non-linear functions, but is susceptible to outliers. Support vector regression (right) can also perform non-linear regression and is more robust against outliers.

$(\varphi(x_1), \ldots, \varphi(x_n))^t$ in Equation (6.3), we obtain the optimal weight vector $w = \Phi(\lambda I_n + \Phi^T \Phi)^{-1} y$. As this is a vector in the only implicitly defined Hilbert space $\mathcal{H}$, we cannot represent w itself. However, we can calculate the kernelized prediction function $f(x)$ as the inner product of w with the image of a test point x under the feature map φ:

$$f(x) = \langle w, \varphi(x) \rangle_{\mathcal{H}} = y(\lambda I_n + K)^{-1} \kappa(x), \tag{6.4}$$

where $K = (k(x_i, x_j))_{i,j=1}^n$ is the kernel matrix of the training data and $\kappa(x) = (k(x_1, x), \ldots, k(x_n, x))^t$ is the vector of kernel values for the test point. Equation (6.4) provides a closed form expression for doing non-linear regression with arbitrary kernel functions.

6.2 Support Vector Regression

Because kernel ridge regression is derived from linear least-squares regression it suffers from some of the same drawback. In particular, the quadratic penalization of the residua makes it very sensitive to outliers,

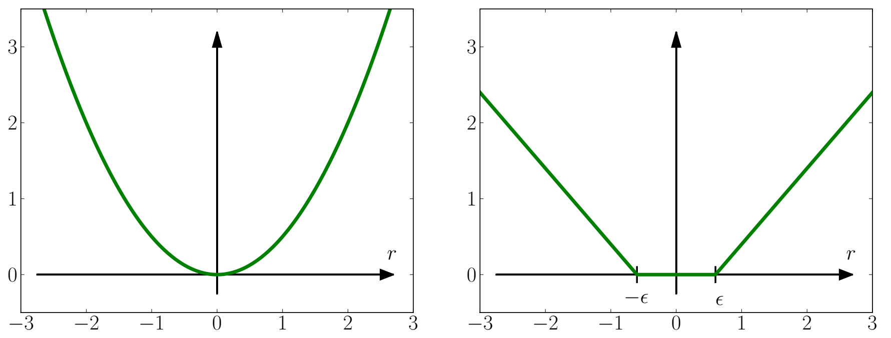

(a) Quadratic penalization function (b) ε-insensitive linear penalization function

Figure 6.2 Penalization of residua: kernel ridge regression (left) uses a quadratic cost $\frac{1}{2}r^2$ function to penalize a residual of r. Support vector regression (right) uses a piece-wise linear penalization $\max(0, |r| - \varepsilon)$ that causes residua of up to $|r| \leq \varepsilon$ not to be penalized at all.

see Figure 6.1. Also, the inverse matrix in Equation (6.4) is generally dense. This means that we have to store all $n(n+1)/2$ unique entries and we have to multiply with a full $n \times n$ matrix to make a prediction. This becomes computationally prohibitive when the number of training samples grows.

As a more robust and sparse non-linear regression technique, *support vector regression (SVR)* has been developed [Drucker et al., 1996]. It can be seen as an adaption of support vector machines to a regression setup. Like kernel ridge regression, support vector regression performs linear regression in an implicit feature space $\mathcal{H}$. However, it uses a different method to penalize the residua: up to a certain tolerance $\varepsilon > 0$, differences between $f(x_i)$ and y_i are not penalized at all. Larger differences are penalized only by their absolute value, not by a quadratic term as Equation (6.2), see Figure 6.2. This makes SVR more robust against outliers.

Mathematically, support vector regression can be termed as the following minimization problem:

$$\min_{\substack{w \in \mathcal{H}, \\ \xi_1,\dots,\xi_n \in \mathbb{R}^+, \\ \xi'_1,\dots,\xi'_n \in \mathbb{R}^+}} \quad \|w\|^2 + C \sum_{i=1}^{n} (\xi_i + \xi'_i) \tag{6.5}$$

subject to

$$y_i - \langle w, \varphi(x_i)\rangle \leq \varepsilon + \xi_i, \qquad \text{for } i = 1, \dots, n, \tag{6.6}$$

$$\langle w, \varphi(x_i)\rangle - y_i \leq \varepsilon + \xi_i', \qquad \text{for } i = 1, \dots, n. \tag{6.7}$$

By use of the Representer Theorem, we obtain $w = \sum_{i=1}^{n} \alpha_i \varphi(x_i)$, which allows us to express the system (6.5)–(6.7) only in terms of kernel function evaluations. A detailed derivation can be found *e.g.* in [Schölkopf and Smola, 2002].

6.3 Example: Pose Estimation

Y. Li, S. Gong, J. Sherrah, and H. Liddell: *"Support Vector Machine based Multi-view Face Detection and Recognition"*, Image and Vision Computing, 2004.

Kernel-based regression has found relatively little application in computer vision research so far. One exception is [Li et al., 2004] that use support vector regression with Gaussian kernel to estimate the pose (yaw and tilt) of faces from single images. The training data consists of face images of known pose as training data that are represented by PCA-coefficients of normalized pixel intensities. At test time, the method exhaustively scans the image, evaluating the learned regression function for each candidate location. Based on the estimated yaw and tilt, different face detection classifiers (frontal or profile) are used to decide if a face is present at the current location.

7

Dimensionality Reduction

Data representations in computer vision are often very high-dimensional. An image treated as a vector can have millions of dimensions and even the most compact histogram representations typically have several hundred entries. This introduces a number of problems for practical applications, in particular high storage and computational requirements. Having a large number of non-informative signal dimensions also makes it more difficult to learn robust classification or regression functions. Finally, high-dimensional data spaces are also problematic, because humans have problems to build an intuitive understanding of such data source, when no suitable visualization techniques is available. Dimensionality reduction techniques can overcome all of these problems by reducing the number of signal dimensions while preserving as much as possible of the original information.

7.1 Kernel Principal Component Analysis

The best known technique for dimensionality reduction is *principal component analysis (PCA)*. It identifies the linear subspace in the feature space in which the data varies strongest. By projecting onto these subspaces, the data is transfered into a low-dimensional coordinate system while retaining the largest possible amount of signal contents.

Mathematically, PCA can be formulated as a maximization problem. We are given a set of data points $x_1, \dots, x_n$ that we assume to have zero mean, *i.e.* $\frac{1}{n}\sum_i x_i = 0$ (we will discuss the general case of $\frac{1}{n}\sum_i x_i \neq 0$ in the later *Data Centering* section). The first PCA coordinate direction w_1 is defined by

$$w_1 = \underset{w \in \mathbb{R}^d,\ \|w\|=1}{\operatorname{argmin}} \sum_{i=1}^{n} \|x_i - \langle x_i, w \rangle w\|^2. \tag{7.1}$$

The squared norm term measures the distortion introduced by projecting a data point x_i to the direction defined by w. Therefore, Equation (7.1) identifies the projection direction w_1 causing the minimal distortion over the whole dataset. To find subsequent PCA projection directions, we solve the same optimization problem as above, but with the additional constraint that every direction w_{k+1} must be orthogonal to all previous $w_1, \dots, w_k$. A classical analysis shows that the first m PCA directions are just the eigenvectors of the m largest eigenvalues of the data covariance matrix $C = \frac{1}{n}\sum_i x_i x_i^t$ [Jolliffe, 1986].

7.1.1 A inner product formulation of PCA

In order to kernelize PCA, we rewrite the problem in terms of inner products. Inserting $C = \frac{1}{n}\sum_i x_i x_i^t$ into the eigenvalue equation $\lambda_k w_k = C w_k$, where λ_k is the k-th eigenvalue of C, we obtain

$$w_k = \frac{1}{n\lambda_k} \sum_{i=1}^{n} \langle x_i, w_k \rangle x_i, \tag{7.2}$$

which shows that any w_k can be written as a linear combination $\sum_i \alpha_i^k x_i$ of the data points, and w_k is completely determined by the coefficient vector $\alpha^k = (\alpha_1^k, \dots, \alpha_n^k)$ built from the inner product values $\alpha_i^k := \frac{1}{n\lambda_k}\langle x_i, w_k \rangle$ for $i = 1, \dots, n$. Inserting w_k back into this expression for α^k, we obtain

$$n\lambda_k \alpha_i^k = \sum_{j=1}^{n} \alpha_j^k \langle x_i, x_j \rangle. \tag{7.3}$$

Since the coefficients α_i^k completely determine the projection direction, we have found a formulation of PCA that only requires information about inner products between data points.

7.1.2 Kernelization

We can now kernelize PCA by replacing all occurrences of the data points x_i by their nonlinearly transformed image $\varphi(x_i) \in \mathcal{H}$, induced by a kernel function k. In result, we obtain a method that performs linear PCA in $\mathcal{H}$, but which is non-linear with respect to the original data space. Using $k(x_i, x_j) = \langle \varphi(x_i), \varphi(x_j) \rangle_{\mathcal{H}}$, Equation (7.3) becomes

$$n\lambda_k \alpha_i^k = \sum_{j=1}^{n} \alpha_j^k k(x_i, x_j), \tag{7.4}$$

showing that $(\alpha^k)_{i=1,\dots,n}$ is an eigenvector of the kernel matrix $K = (k(x_i, x_j))_{i,j=1}^n$ with corresponding eigenvalue $n\lambda_k$. Having computed $\alpha_1, \dots, \alpha_m$, we obtain the lower-dimensional coordinates $\tilde{x}_i \in \mathbb{R}^m$ for any x_i by the projection coefficient of $\varphi(x_i)$ to the kernelized $w_1, \dots, w_m$. By means of $w_k = \sum_j \alpha_j^k \varphi(x_j)$ this is

$$[\tilde{x}_i]_k = \langle \varphi(x_i), w_k \rangle \;=\; \sum_{j=1}^{n} \alpha_j^k \langle \varphi(x_i), \varphi(x_j) \rangle \;=\; n\lambda_k \alpha_i^k, \tag{7.5}$$

where in the last step we have made use of Equation (7.4).

Equation (7.5) shows that, despite the rather technical derivation, kernel-PCA is very easy to apply in practice: the low-dimensional data matrix $\tilde{X} = [\tilde{x}_1, \dots, \tilde{x}_n]^t \in \mathbb{R}^{n \times m}$ can be calculated by finding the top m eigenvectors of the kernel matrix $K \in \mathbb{R}^{n \times n}$ and multiplying each eigenvector by its corresponding eigenvalue. As an additional bonus, kernel-PCA allows us to derive vector representation for input data that does not have a linear structure by itself, *e.g.* graphs or sequences.

7.1.3 Data Centering

For the sake of clarify, we have ignored one condition of our original PCA formulation in the previous discussion, namely that the data points must have a mean of 0. If the data coordinates are explicitly available, this condition is easily established by *centering* the data, *i.e.* subtracting the data mean $\mu = \frac{1}{n}\sum_{i=1}^{n} x_i$ from each data point. Centering corresponds to a global translation of all points and therefore does not affect our intuition of identifying the directions of maximal data variance.

In the kernelized situation, we do not have access to an explicit coordinate representation of the data points $\varphi(x_i)$, and we can therefore not modify them individually to make the data set have zero mean. However, we can calculate the kernel values $\overline{k}$ that correspond to the inner product values between the embedded data points if they had been centered by subtracting their mean $\mu = \frac{1}{n}\sum_{i=1}^{n} \varphi(x_i)$:

$$\overline{k}(x_i, x_j) = \langle \varphi(x_i) - \mu, \varphi(x_j) - \mu \rangle \tag{7.6}$$

$$= \Big\langle \varphi(x_i) - \frac{1}{n}\sum_{k=1}^{n} \varphi(x_k)\,, \varphi(x_j) - \frac{1}{n}\sum_{l=1}^{n} \varphi(x_l) \Big\rangle \tag{7.7}$$

$$= k(x_i, x_j) - \frac{1}{n}\sum_{k=1}^{n} k(x_k, x_j) - \frac{1}{n}\sum_{l=1}^{n} k(x_i, x_l) + \frac{1}{n^2}\sum_{k=1}^{n}\sum_{l=1}^{n} k(x_k, x_l). \tag{7.8}$$

Thus, we can perform kernel-PCA for any kernel matrix K by first computing the *centered kernel matrix*

$$\overline{K} = K - \frac{1}{n}\mathbf{1}_n K - \frac{1}{n} K\,\mathbf{1}_n + \frac{1}{n^2}\mathbf{1}_n K\,\mathbf{1}_n, \tag{7.9}$$

where $\mathbf{1}_n$ is the $n \times n$ matrix of all ones, and applying the eigenvector decomposition of the previous section to it.

7.2 Kernel Discriminant Analysis

As an unsupervised technique, PCA only uses the variance of the data as indicator what projection directions are most informative. If *label information* is available as part of the training data, *linear discriminant analysis (LDA)* is often a better choice. It identifies the m-dimensional subspace that best separates points of different class membership while grouping together points that belong to the same class.

Mathematically, LDA maximizes the ratio of *between-class scatter* and *within-class scatter*. For a dataset consisting of a part $X^+ =$

$(x_1^+,\dots,x_{n^+}^+)$ with positive class label and a part $X^- = (x_1^-,\dots,x_{n^-}^-)$ with negative class label, the first LDA projection direction is given by

$$w_1 = \underset{w\in\mathbb{R}^d,\ \|w\|=1}{\operatorname{argmax}} \quad \frac{w^t\Sigma_b w}{w^t\Sigma_w w} \tag{7.10}$$

where $\Sigma_b = (\mu^+ - \mu^-)(\mu^+ - \mu^-)^t$ is the between-class scatter matrix, $\Sigma_w = \sum_{i=1}^{n^+}(x_i^+ - \mu^+)(x_i^+ - \mu^+)^t + \sum_{i=1}^{n^-}(x_i^- - \mu^-)(x_i^- - \mu^-)^t$ is the sum of within-class scatter matrices, and $\mu^\pm = \frac{1}{n_\pm}\sum_{i=1}^{n^\pm} x_i^\pm$ denote the positive and negative class means [McLachlan, 1992]. The optimization problem (7.10) can be solved efficiently by means of a generalized eigenvalue problem. As for PCA, more projection directions can be found by optimizing the same expression with additional constraints that any new direction must be orthogonal to all previous ones.

7.2.1 Kernelization

LDA can be kernelized by similar calculations as were required for PCA resulting in *kernel discriminant analysis (KDA)* [Mika et al., 1999]. Instead of Σ_b, we need to form $M = (M_+ - M_-)(M_+ - M_-)^t$ with $[M_\pm]_j = \frac{1}{n^\pm}\sum_{i=1}^{\pm} k(x_j, x_i^\pm)$ for $j = 1,\dots,n$ and slightly abusing the notation such that $X^+ \cup X^- = \{x_1,\dots,x_n\}$. The role of Σ_w is taken over by $N = K_+(I_{n^+} - \frac{1}{n^+}\mathbf{1}_{n^+})K_+^t + K_-(I_{n^-} - \frac{1}{n^-}\mathbf{1}_{n^-})K_-^t$ where $(K_\pm)_{ij} = k(x_i, x_j^\pm)$ for $i = 1,\dots,n$ and $j = 1,\dots,n^\pm$. With this notation, the solution $\alpha = (\alpha_1,\dots,\alpha_n)$ of the maximization problem

$$\underset{\alpha\in\mathbb{R}^n}{\operatorname{argmax}} \frac{\alpha^t M\alpha}{\alpha^t N\alpha} \tag{7.11}$$

yields the coefficients of the expansion $w_1 = \sum_{i=1}^n \alpha_i^k\varphi(x_i)$. As in the case of PCA, more projection directions can be found by maximizing equation (7.11) with additional orthogonality constraints.

7.3 Kernel Canonical Correlation Analysis

Canonical correlation analysis (CCA) generalizes PCA to the situation of *paired data*, *i.e.* a dataset $X = \{x_1,\dots,x_n\}$ where all samples are available in (at least) two representation at the same time: $\{x_1^1,\dots,x_n^1\} \subset \mathcal{X}^1$ and $\{x_1^2,\dots,x_n^2\} \subset \mathcal{X}^2$ with known correspondences between x_i^1 and x_i^2 for $i = 1, \dots, n$ [Hotelling, 1936]. CCA learns separate projections from each data domain $P^1 : \mathcal{X}^1 \to \mathbb{R}^m$ and $P^2 : \mathcal{X}^2 \to \mathbb{R}^m$ such that the low-dimensional representations $\{P^1(x_i^1)\}_{i=1,\dots,n}$ and $\{P^2(x_i^2)\}_{i=1,\dots,n}$ are maximally correlated. If $\mathcal{X}^2 = \{-1, 1\}$, CCA reduces to LDA. Therefore, CCA can also be thought of as a generalization of LDA, where instead of a binary label y_i only a second data representation x_i^2 is available.

7.3.1 Kernelization

Directly kernelizing linear CCA with kernels $k_1 : \mathcal{X}^1 \times \mathcal{X}^1 \to \mathbb{R}$ and $k_2 : \mathcal{X}^2 \times \mathcal{X}^2 \to \mathbb{R}$ yields degenerate projection directions if either of the kernel matrices K_1 or K_2 is invertible. One overcomes this by regularizing the problem, resulting in the following maximization task:

$$\operatorname*{argmax}_{\alpha\in\mathbb{R}^n, \beta\in\mathbb{R}^n} \frac{\alpha^t K_1 K_2 \beta}{\sqrt{\alpha^t K_1^2 \alpha + \epsilon_1 \alpha^t K_1 \alpha}\sqrt{\beta^t K_2^2 \beta + \epsilon_2 \beta^t K_2 \beta}}, \tag{7.12}$$

where $\epsilon_1, \epsilon_2 > 0$ are regularization parameters [Lai and Fyfe, 2000].

As for LDA, the solutions to Equation (7.12) can be found by a generalized eigenvalue problem, which yields projection directions of maximal correlation: $w_1 = \sum_{i=1}^n \alpha_i \varphi_1(x_i^1)$ and $w_2 = \sum_{i=1}^n \beta_i \varphi_2(x_i^2)$. The lower-dimensional representations can also be calculated directly as $P(x) = \sum_{i=1}^n \alpha_i k_1(x, x_i^1)$ for $x \in \mathcal{X}^1$ and $Q(x) = \sum_{i=1}^n \beta_i k_2(x, x_i^2)$ for $x \in \mathcal{X}^2$. As before, further projection directions can be computed by searching for solutions orthogonal to the earlier α and β. This procedure is equivalent to searching for the generalized eigenvectors corresponding to the largest m eigenvalues.

7.4 Example: Image Denoising

S. Mika, B. Schölkopf, A. Smola, K.-R. Müller, M. Scholz, G. Rätsch: *“Kernel PCA and De-Noising in Feature Spaces”*, NIPS 1999

[Mika et al., 1999] propose kernel-PCA for image denoising. Similar to PCA-based linear denoising approaches, the method works by projecting the image onto few principal components and considering the remaining components as the noise part of the image. In contrast to denoising with linear PCA, kernelized denoising is non-trivial, because in the low-dimensional representations found by kernel-PCA the data points do not directly correspond to images again. Instead, they are vectors in the implicitly defined feature space. To obtain an actual denoised version of an image, the authors solve a *preimage problem*, *i.e.* they find the image x such that $\varphi(x)$ best approximates the latent feature space representation. Examples from the USPS dataset of handwritten digits show superior performance of the proposed method compared to linear PCA denoising.

It is noteworthy that [Kwok and Tsang, 2004] later introduced a different optimization technique for solving the kernel-PCA preimage problem for certain kernel types, achieving improved denoising results and higher numerical stability.

7.5 Example: Face Recognition

M. H. Yang: *Kernel eigenfaces vs. kernel fisherfaces: Face recognition using kernel methods*, IEEE Conference on Automatic Face and Gesture Recognition 2002

Motivated by the fact that many successful techniques for face recognition rely on linear dimensionality reduction, [Yang, 2002] applies kernel-PCA and KDA to face images, thereby generalizing *eigenfaces* [Turk and Pentland, 1991] to *kernel-eigenfaces*, and *fisherfaces* [Belhumeur et al., 1997] to *kernel-fisherfaces*. Using a polynomial or Gaussian kernel, the kernelized methods showed higher accuracy on standard face recognition datasets than their linear counterparts, and also than other classical dimensionality reduction techniques such as *independent component analysis* (ICA) or *locally linear embedding* (LLE).

8

Clustering

Clustering is a classical method for the detection of structure in large and unlabeled datasets. It partitions the data into a small number of groups of samples, typically based on their distances to a centroid or on pairwise similarities. In the following we introduce three clustering methods that rely on kernels for this task: *kernel-PCA clustering*, *kernel vector quantization* and *support vector clustering*.

8.1 Kernel-PCA Clustering

Possibly the most popular clustering technique is the K-means algorithm [MacQueen, 1967] that identifies a set of K centroids[1] $c_1, \dots, c_K$ with the goal of minimizing the L^2 distortion caused if each sample is replaced by the centroid it lies closest to:

$$\operatorname*{argmin}_{c_1,\dots,c_K \in \mathbb{R}^d} \quad \sum_{i=1}^{n} \min_{j=1,\dots,K} \|x_i - c_j\|^2. \tag{8.1}$$

[1] We use the letter K to denote the number of cluster centroids, because it is has become an established part of the name "K-means". It is, of course, not to be confused with the kernel matrix, which we will not need as a dedicated object in this chapter.

K-means clustering requires only calculations of the distance between samples and prototype vectors and of the mean vector for finite sets of samples. It can therefore be kernelized in a straight forward way, see [Girolami, 2002]. However, in contrast to the situation in $\mathbb{R}^d$, the resulting centroids c_k in the implicit Hilbert space induced by the kernel function cannot be represented explicitly. We know them only in form of a linear combinations of the data points: $c_k = \sum_j \alpha_j^k \varphi(x_j)$. Consequently, each distance calculation between a prototype and a data sample requires many evaluations of the kernel function. In combination with the iterative nature of the K-means procedure, many such calculations are required before convergence, which makes kernelized K-means a computationally expensive procedure.

As a more efficient approximation, *kernel-PCA clustering* has been proposed. It makes use of the fact that *kernel-PCA* can find an explicit vector representation of the dataset that approximates the kernel-defined inner products and thereby the distances between samples. This allows us to come up with an efficient two-step clustering procedure:

Kernel-PCA Clustering. Let $X = \{x_1, \dots, x_n\} \subset \mathcal{X}$ be a dataset to be clustered and $k : \mathcal{X} \times \mathcal{X} \to \mathbb{R}$ a kernel function.

(1) Perform kernel-PCA on the dataset, obtaining a vector representation $\hat{x}_1, \dots, \hat{x}_n \in \mathbb{R}^m$.
(2) Apply ordinary K-means clustering to the vectors $\hat{x}_1, \dots, \hat{x}_n$.

Because *kernel-PCA clustering* is very easy to implement and computationally efficient, it has become one of the most popular methods for clustering with a non-linear distance functions. Figures 8.1 and 8.2 illustrate its working principle.

8.2 Kernel Vector Quantization

Like most clustering algorithms, *K-means* and *kernel-PCA clustering*, treat the number of clusters as a free parameter. Only after this value has been specified, the algorithms determines the centroids minimizing the total distortion if all samples are quantized to their closest centroid. *Learned Vector Quantization (LVQ)* is a clustering method that takes

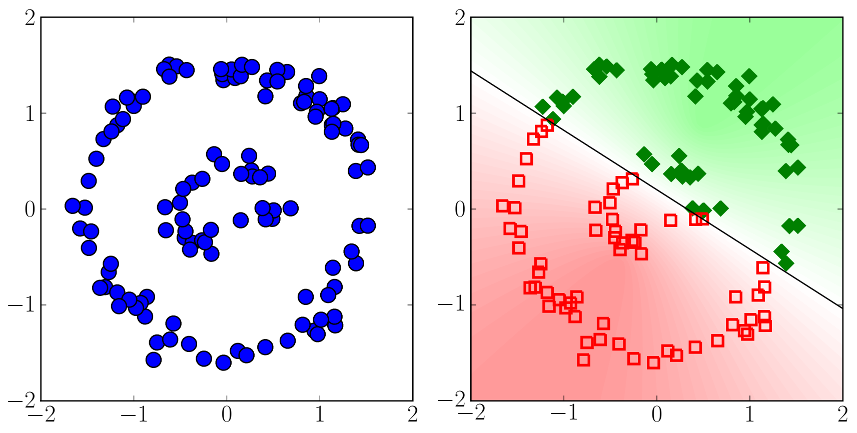

(a) *Two Rings* dataset (b) Result of K-means clustering

Figure 8.1 K-means fails to clusters if they are linearly separable (left), because it can only model linear decision boundaries between clusters (right).

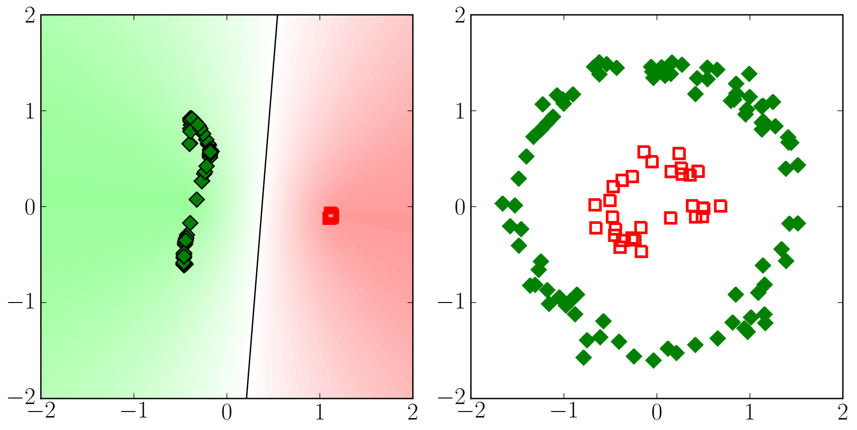

(a) K-means in kernel-PCA space (b) resulting kernel-PCA clustering

Figure 8.2 Preprocessing the *two rings* dataset with *kernel-PCA* (here with *commute distance* kernel) creates a representation of the dataset with clearly separated cluster structure (left). Clustering this representation with K-means results in a perfect separation of the intended data clusters (right).

a dual approach to this: for a fixed maximal distance θ, it determines how many and which centroids are necessary in order to ensure that the distance between any samples and its nearest centroid does not exceed the value θ. By choosing the centroids as a subset of the data

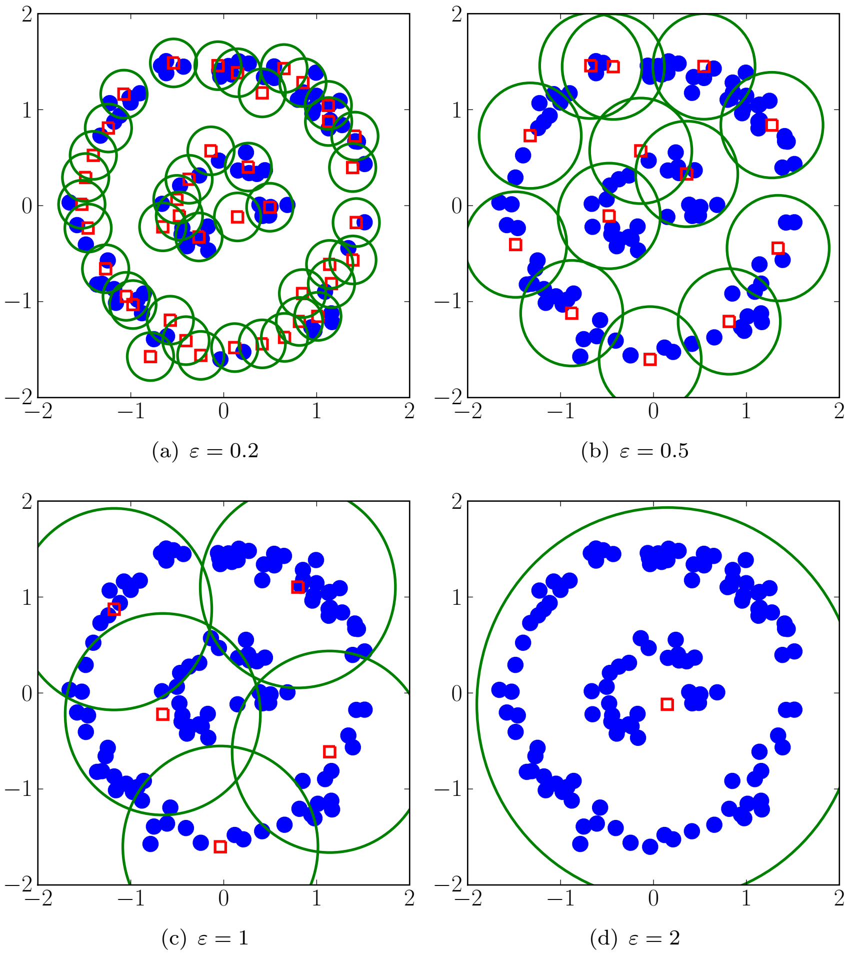

Figure 8.3 (Kernel) vector quantization. For any value $\theta > 0$, one identifies prototypes that provide a minimal covering of the data set by balls of radius θ. The larger the radius, the fewer prototypes are required.

points instead of linear combinations, one can formulate the problems as a boolean optimization problem:

$$\underset{z_1,\dots,z_n\in\{0,1\}}{\operatorname{argmin}} \sum_{i=1}^{n} z_i \quad \text{subject to} \quad \sum_{i=1}^{n} z_j d_{ij} \geq 1 \quad \text{for } j = 1,\dots,n, \tag{8.2}$$

where $d_{ij} = 1$ if $\|x_i - x_j\| \leq \theta$ and $d_{ij} = 0$ otherwise. The resulting variables z_i are indicators whether the data point x_i is required as a centroid or not. Clusters are formed subsequently by assigning each data point to the cluster centroid it lies closest to, see Figure 8.3.

An interesting aspect of the above optimization problem is the fact that the samples x_i only appear in it through their thresholded pairwise distances d_{ij}. This allows us to kernelize LVQ by replacing the Euclidean distance by the distance in a Hilbert space $\mathcal{H}$ induced by a kernel function k. These distances can be expressed solely by kernel evaluations:

$$\begin{aligned}\|\varphi(x_i)-\varphi(x_j)\|^2_{\mathcal{H}} &= \langle \varphi(x_i)-\varphi(x_j), \varphi(x_i)-\varphi(x_j)\rangle_{\mathcal{H}} \\ &= \langle \varphi(x_i), \varphi(x_i)\rangle_{\mathcal{H}} - 2\langle \varphi(x_i), \varphi(x_j)\rangle_{\mathcal{H}} + \langle \varphi(x_j), \varphi(x_j)\rangle_{\mathcal{H}} \\ &= k(x_i, x_i) - 2k(x_i, x_j) + k(x_j, x_j), \qquad (8.3)\end{aligned}$$

which allows us to calculate a kernelized version of the matrix d_{ij} directly from the entries of the kernel matrix. The resulting procedure is called *kernel vector quantization (KVQ)*.

To allow the solution of large problems, one typically convexifies the optimization problem by relaxing the constraints $z_i \in \{0, 1\}$ to $z_i \in [0, 1]$. The result is a *linear program*, which can be solved efficiently even for tens of thousands of samples. However, the result might have more non-zero z_i, and therefore centroids, than necessary. Different postprocessing operations and iterative schemes have been proposed to bring the related solution closer to the optimal binary one [Tipping and Schölkopf, 2001; Weston et al., 2003].

8.3 Support Vector Clustering

Support vector clustering (SVC) [Ben-Hur et al., 2002] differs from *K-means* and *vector quantization* based techniques in that it does not define clusters by a set of prototypes. Instead, it relies on the fact that the feature mapping $\varphi : \mathcal{X} \to \mathcal{H}$ induced by a Gaussian kernel $k : \mathcal{X} \times \mathcal{X} \to \mathbb{R}$ is topologically non-trivial, *i.e.* φ can map regions that are far apart in the original space to nearby locations in the kernel induced feature space $\mathcal{H}$. SVC works by first applying *support vector data description* with a Gaussian kernel on the dataset. While in the latent feature space the resulting *inlier region* is just a ball B, the corresponding region $\varphi^{-1}(B)$ in the original data space is non-linearly

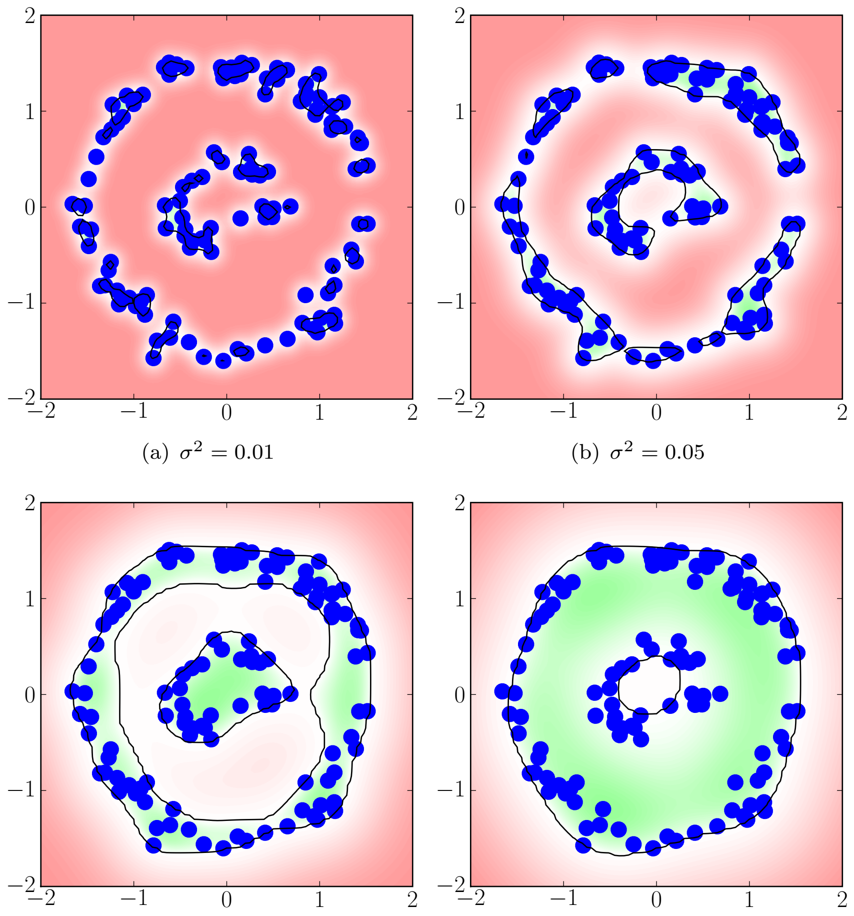

(a) $\sigma^2 = 0.01$ (b) $\sigma^2 = 0.05$

(c) $\sigma^2 = 0.2$ (d) $\sigma^2 = 0.5$

Figure 8.4 Support vector clustering (Gaussian kernel, $\nu = 0.05$). For small bandwidth parameters σ^2, many small clusters are identified. When σ^2 is increased, the decision boundary becomes smoother and fewer but larger clusters are formed.

distorted and often consists of multiple components. SVC defines each connected component of the inlier region to be one data cluster, *i.e.* two data points are assigned the same cluster label, if there is a path in the original data space connecting them without leaving the inlier region $\varphi^{-1}(B)$. By this construction, the number of clusters that SVC identifies is not determined a priori, but it results from the distribution of data points in the data space. However, the Gaussian's bandwidth parameter can be used to influence on the number of clusters, as a smaller bandwidth causes the preimage $\varphi^{-1}(B)$ to be more irregular and less connected, see Figure 8.4. By use of SVDD's ν-parameter, SVC is one of the few clustering methods that can deal with outliers in the data, as it assigns no cluster label to those points.

8.4 Example: Unsupervised Object Categorization

T. Tuytelaars, C. H. Lampert, M. B. Blaschko, W. Buntine: *"Unsupervised Object Discovery: A comparison"*, IJCV 2009.

In order to automatically detect object categories in images collections, Tuytelaars et al. [2009] compare different centroid-based clustering methods with probabilistic topic models. With images represented by bag of visual words histograms, kernel-PCA clustering and the related *spectral clustering* [Belkin and Niyogi, 2003] with χ^2 kernel were found superior to ordinary k-means clustering, with or without linear PCA as preprocessing technique, and to generative topic models.

8.5 Example: Clustering of Multi-Modal Data

M. B. Blaschko, and C. H. Lampert: *"Correlational Spectral Clustering"*, CVPR 2008.

In many computer vision task, data is available in more than one modality, *e.g.* images with text captions. [Blaschko and Lampert, 2008a] introduce *Correlational Spectral Clustering (CSC)*, a technique that generalizes kernel-PCA clustering to data source that come in multiple representations. CSC consists of kernel-CCA for dimensionality reduction followed by K-means for the clustering step. Experiments showed superior performance of clustering with kernel-CCA based preprocessing compared to linear CCA and to PCA or kernel-PCA based methods that do not take the information of multiple modalities into account.

9 Non-Classical Kernel Methods

Support vector clustering in the previous chapter was our first example of a kernel method that did not have a linear counterpart, because it explicitly required a non-linear feature mapping in order to give meaningful results. In this section, we study two more concepts that crucially rely on the rich and often infinite-dimensional structure of induced Hilbert spaces, the *prediction of structured objects* and the *empirical Hilbert-Schmidt independence criterion (HSIC)*.

9.1 Structured Prediction

Classical kernel methods like classification and regression learn mappings $\mathcal{X} \to \{1, \dots, M\}$ and $\mathcal{X} \to \mathbb{R}$, where $\mathcal{X}$ is an arbitrary set, provided we can define a kernel over it. However, many realistic problems require decisions on several quantities at once, *e.g.* in pixel-wise image segmentation, or in the prediction of richly structured objects like interaction graphs. Such tasks can be subsumed under the label of *structured prediction*, where the problem consists of learning a prediction function $F : \mathcal{X} \to \mathcal{Y}$ for any suitable $\mathcal{Y}$.

9.1.1 Structured Support Vector Machines

The *structured (output) support vector machine (S-SVM)* [Tsochantaridis et al., 2005] provides an extension of SVM classification to structured prediction problems. Its key idea is to define a *joint kernel function*

$$k_{joint} : (\mathcal{X} \times \mathcal{Y}) \times (\mathcal{X} \times \mathcal{Y}) \to \mathbb{R} \tag{9.1}$$

between two *(sample,label)*-pairs, and learn a kernelized *compatibility function* $f : \mathcal{X} \times \mathcal{Y} \to \mathbb{R}$ based on this, where $f(x, y) = \langle w, \Phi(x, y)\rangle_{\mathcal{H}}$ is a linear function in the feature space $\mathcal{H}$ induced by k_{joint} with latent feature map $\Phi : \mathcal{X} \times \mathcal{Y} \to \mathcal{H}$. Subsequently, a structured prediction function $F : \mathcal{X} \to \mathcal{Y}$ is obtained by maximizing the compatibility between any test input x and all possible outputs y:

$$F(x) := \operatorname*{argmax}_{y \in \mathcal{Y}} f(x, y). \tag{9.2}$$

9.1.2 Structured SVM Training

Structured support vector machines are trained using a maximum-margin principle similar to the ordinary SVM training procedure. For a given training set $\{(x_1, y_1), \dots, (x_n, y_n)\}$, one solves the convex optimization problem

$$\min_{\substack{w \in \mathcal{H}, \\ \xi_1,\dots,\xi_n \in \mathbb{R}^+}} \|w\|^2 + \frac{C}{n} \sum_{i=1}^{n} \xi_i \tag{9.3}$$

subject to the margin constraints[1]

$$\langle w, \Phi(x_i, y_i)\rangle_{\mathcal{H}} - \langle w, \Phi(x_i, y)\rangle_{\mathcal{H}} \geq \Delta(y, y_i) - \xi_i, \quad \text{for all } y \neq y_i, \tag{9.4}$$

for $i = 1, \dots, n$. Similarly to the Crammer-Singer multiclass SVM (4.4), the constraints (9.4) enforce a margin for each training example x_i

[1] More precisely, the constraints (9.4) define a structured SVM *with margin-rescaling.* The variant of *slack rescaling*, which is also proposed in [Tsochantaridis et al., 2005], uses the constraints

$$\langle w, \Phi(x_i, y_i)\rangle_{\mathcal{H}} - \langle w, \Phi(x_i, y)\rangle_{\mathcal{H}} \geq \Delta(y, y_i)(1 - \xi_i) \quad \text{for all } y \neq y_i,$$

for $i = 1, \dots, n$. This has some theoretical advantages but is used less frequently in practice, because the resulting optimization problem is more difficult to solve.

between the correct label y_i and any other label $y \neq y_i$. However, in contrast to the multiclass situation, the margin is not of constant size 1, but it is determined by a *loss function* $\Delta : \mathcal{Y} \times \mathcal{Y} \to \mathbb{R}^+$. This allows one to integrate the fact that in a structured output space some output values y, even if not completely correct, are still "less wrong" than others and should therefore not be penalized as strongly. In an image segmentation problem, Δ could *e.g.* express the difference between a segmentation in which one pixel is wrong, and a segmentation in which all pixels are wrong.

The joint kernel function k_{joint} also generalizes the multiclass situation, which we can recover by setting

$$k_{multiclass}(\,(x,y)\,,(x',y')\,) = k_x(x,x')\delta_{y=y'} \tag{9.5}$$

for any kernel k_x over $\mathcal{X}$, where $\delta_{y=y'} = 1$ is $y = y'$ and $\delta_{y=y'} = 0$ otherwise. The greater flexibility in choosing k_{joint} allows the formulation of many computer vision problems in terms of a structured SVM that before were mainly treated by heuristic or only locally optimal techniques.

9.2 Dependency Estimation

An important question in data analysis is to determine whether two measured quantities are independent of each other. Mathematically, one studies this by treating the two sets of measurements $X = \{x_1, \ldots, x_n\}$ and $Y = \{y_1, \ldots, y_n\}$ as realization of random variables $\mathbf{x}$ and $\mathbf{y}$ and trying to determine if their joint probability distribution function factorizes, *i.e.* if $p(\mathbf{x}, \mathbf{y}) = p(\mathbf{x})\, p(\mathbf{y})$.

Elementary techniques for this task measure dependence by calculating *data moments*, in particular the *sample covariance* or *correlation* matrices. However, while correlation between two random quantities implies their statistical dependence, the converse is not true: two uncorrelated random variables can still be connected by strong dependence, see Figure 9.1 for an illustration.

One way to overcome this problem is the introduction of nonlinearity: a classical result by Rényi states that two random variable $\mathbf{x}$ and $\mathbf{y}$ are independent if and only if all transformed variables $f(x)$ and

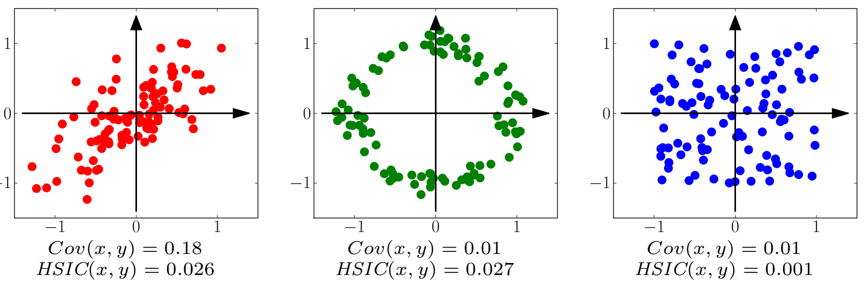

Figure 9.1 Covariance vs. dependence. Left: the samples have correlated, and therefore dependent, x and y coordinates. This is reflected by non-zero values of both the *covariance coefficient* $Cov(x, y)$ and by the empirical *Hilbert-Schmidt independence criterion* $HSIC(x, y)$. Center: the coordinates of the samples are dependent, because for each x, only certain values occur for y. The *covariance coefficient* of these sample, however, is almost 0, whereas *HSIC* correctly picks up on the dependence and yields an as large score as in the correlated case. Right: the samples on the right have independent x and y coordinates. *Covariance* and *HSIC* both nearly vanish.

$g(y)$ are uncorrelated, where f and g range over all bounded continuous functions $f : \mathcal{X} \to \mathbb{R}$ and $g : \mathcal{Y} \to \mathbb{R}$ [Rényi, 1959].

9.2.1 Hilbert-Schmidt Independence Criterion

Clearly, it is not possible to calculate $cov(f(\mathbf{x}), g(\mathbf{y}))$ for all possible functions f and g. However, in the following we will see that by using kernels we can do so *implicitly*.

Definition 9.1. Let $k_x : \mathcal{X} \times \mathcal{X} \to \mathbb{R}$ and $k_y : \mathcal{Y} \times \mathcal{Y} \to \mathbb{R}$ be two *characteristic*[2] kernel functions. Then, an estimate of the statistical dependency between two modalities X and Y of a paired dataset $Z = \{(x_1, y_1), \ldots, (x_n, y_n)\}$ is given by the *empirical Hilbert-Schmidt independence criterion (HSIC)* [Fukumizu et al., 2008]:

$$HSIC_{emp}(Z; k_x, k_y) := \frac{1}{(n-1)^2} \operatorname{trace} \overline{K}_x \overline{K}_y \tag{9.6}$$

where $\overline{K}_x$ and $\overline{K}_y$ are the centered versions of the kernel matrices $K_x = k_x(x_i, x_j)_{i,j=1,\ldots,n}$, $K_y = k_y(y_i, y_j)_{i,j=1,\ldots,n}$.

[2] The definition of *characteristic* kernels is rather technical, see [Fukumizu et al., 2008]. However, many kernels popular in computer vision are of this class, *e.g.* Gaussian and χ^2-kernels and all universal kernels over compact domains.

The relevance of the empirical HSIC score follows from the fact that $HSIC_{emp}(Z; k_x, k_y)$ is a consistent estimator of the *Hilbert Schmidt independence criterion* $HSIC(p(\mathbf{x},\mathbf{y})\,; k_x, k_y)$ for the probability density $p(\mathbf{x},\mathbf{y})$ according to which the data sets X and Y were generated. $HSIC(p(\mathbf{x},\mathbf{y})\,; k_x, k_y)$ can be shown to vanish if and only if $\mathbf{x}$ and $\mathbf{y}$ are independent random variables [Fukumizu et al., 2008].

The derivation of HSIC and the proof of the statements are beyond the scope of this work, but its consequences will prove useful also for practical application in computer vision. In particular, *HSIC* provides us with a tool to compare two datasets in terms of the *randomness* of their pairing without need for a similarity measure that compares elements $x \in \mathcal{X}$ with elements $y \in \mathcal{Y}$.

9.3 Example: Image Segmentation

D. Anguelov, B. Taskar, and V. Chatalbashev: *"Discriminative Learning of Markov Random Fields for Segmentation of 3D Scan Data"*, CVPR 2005.

Maximum-margin trained structured prediction models were introduced into the field of computer vision by [Anguelov et al., 2005]. They formulate the task of terrain classification as a graph labeling problem: each sample point of a 3D laser scan is a node in a graph, to which a region label has to be assigned, *e.g. ground, building* or *tree*. The authors train a *maximum margin Markov network* (M^3N) [Taskar et al., 2003], which can be seen as a structured SVM with special choice of the loss function. Training and prediction are done using *min-cut with α-expansion* [Boykov and Kolmogorov, 2004], achieving higher segmentation accuracy than per-site SVMs, and that an SVM with a label smoothing step as post-processing.

[Szummer et al., 2008] later used a similar approach for 2D image segmentation relying on the 4-connected graph over all image pixels. Training a structured SVM for the resulting graph labeling problem, they achieved better segmentation accuracy than with a probabilistically trained *conditional random field* (CRF) [Lafferty et al., 2001].

9.4 Example: Object Localization

M. B. Blaschko, C. H. Lampert: *"Learning to Localize Objects by Structured Output Regression"*, ECCV 2008.

[Blaschko and Lampert, 2008b] formulate the task of object localization in natural images as a structured prediction task, in which one learns a function from the set of images to the set of bounding box coordinate tuples. In order to compare images with such bounding box annotation the authors introduce a joint kernel function called *restriction kernel*. Using a linear kernel for bag of visual word histograms, structured SVM training and prediction can be performed using an efficient branch-and-bound technique [Lampert et al., 2008, 2009]. Experiments on standard datasets for object localization show that the S-SVM yields more accurate localization than previous approaches that used the decision function of a binary SVM for sliding window localization.

9.5 Example: Image Montages

N. Quadrianto, L. Song and A. J. Smola: *"Kernelized Sorting"*, NIPS 2008.

Arranging images in two- or three-dimensional layouts is a useful tool for image screening and visualization. [Quadrianto et al., 2008] propose *Kernelized Sorting*, a method that allows the optimal arrangement of image datasets in an arbitrary output pattern, *e.g.* on a regular grid, with respect to a kernel function. The method works by finding the matching between images and grid points that maximizes the empirical *HSIC* score between the image set and the grid points. Since an exact solution to this assignment problem is NP-hard, the authors derive an approximate scheme based on DC programming [Horst and Thoai, 1999].

10

Learning the Kernel

All kernel methods we have seen so far make use of a single fixed kernel function. However, because different kernel functions induce different feature space embeddings and are therefore differently well suited for a given problem, it is natural to ask the question which is the *best kernel function*. Ultimately, this is task dependent, because the *quality* of a kernel is determined by how well the trained kernel method performs in the task at hand, *e.g.* in the case of a classifier by the accuracy on future data points. As we cannot use this quantity directly at training time, many estimators for the generalization error have been developed and used for parameter selection, *e.g.* *cross-validation* and *bootstrapping*, that work by iterating between training and test procedures on different parts of the training set.

In some situations, however, it is not possible to exhaustively explore which kernels or parameters work best, and algorithmic proxies have been developed. For kernels that come from parameterized families, *e.g.* Gaussian kernels with adjustable bandwidth parameter, *kernel target alignment* provides a way to determine good parameters. Alternatively, if a finite set of possible kernels has been preselected, *e.g.* by a human expert, and we want to find a reasonable subset and weights to use for a linear combination of kernels, then *multiple kernel learning* provides an answer. The latter case thereby generalizes *feature selection*, which is the special case that each base kernel functions depend on only one of several available feature types.

For simplicity of the discussion, in the following we will restrict ourselves to classification problems.

10.1 Kernel Target Alignment

The idea of *kernel target alignment (KTA)* [Cristianini et al., 2001] is that the values of a good kernel function $k : \mathcal{X} \times \mathcal{X} \to \mathbb{R}$ should resembled the values of a (hypothetical) "perfect" kernel $l : \mathcal{X} \times \mathcal{X} \to \mathbb{R}$ that has access to the data labels, *i.e.* $l(x, x') = 1$ for any samples x, x' having the same class label, and $l(x, x') = -1$ otherwise. To measure how close k is to the optimal l, we introduce the *kernel alignment score*

$$A(Z; k, l) = \frac{\operatorname{trace}(KL)}{n\sqrt{\operatorname{trace} KK}} \tag{10.1}$$

where $Z = \{(x_1, y_1), \ldots, (x_n, y_n)\}$ is a labeled training set, K is the kernel matrix of k on Z, and L is the kernel matrix induced by the labels[1].

To select one kernel function out of a set of alternatives, we choose the kernel function that maximizes $A(Z; k, l)$. Since this procedure does not require to train and evaluate a classifier, it is in particular faster than multiple cross-validation runs. A further advantage of the kernel alignment score is its differentiability with respect to the kernel function k. For kernels that depend smoothly on real-valued parameters, it it therefore possible to find locally optimal parameters combinations by gradient-ascent optimization.

10.2 Multiple Kernel Learning

As we saw in the *Kernels for Computer Vision* part, coming up with many reasonable kernel functions is often easy, but it is *a priori* unclear

[1] A comparison with Equation (9.6) shows that Equation (10.1) resembles a normalized HSIC measure of dependence between the samples x_i and the labels y_i, but without prior centering of the kernel matrices.

which one is most suitable for the problem, or if there even is a single best one. In computer vision, this question is often related to the choice of representations and features: depending on the application or even on the specific class in a multiclass problem, color, texture, or edge orientation might be the most relevant cue. Most often, however, one finds that different aspects are important at the same time, and one would like to find a kernel function that reflects the aspects of several features at the same time.

Kernel methods are specifically well suited for such feature combination ideas: as we saw in the Section *"Constructing Kernel Functions"*, the sum and product of existing kernels are kernels again, reflecting the properties of all base kernel at the same time. However, in situations, where we believe that some kernels are more important than others, we might prefer a *weighted linear combination* of kernel instead of just their unweighted sum. *Multiple kernel learning (MKL)* allows us to find the weights of such a linear combination[2]. It is based on the idea that each kernel or combination of kernels gives rise to a *margin* when used in the training of a support vector machine, and due to the linear kernel combination, we can find an explicit expression for the size of the margin. Because the concept of maximum margin learning tells us to prefer classifiers with a large margin between the classes, the MKL procedure jointly finds the SVM weight vector and the linear combination weights of the kernel functions that realizes the generalized linear classifier of maximal margin, see Figure 10.1 for an illustration.

10.2.1 Linear Kernel Combinations

Let $k_1, \dots, k_m$ be kernel functions, $k_j : \mathcal{X} \times \mathcal{X} \to \mathbb{R}$, with induced Hilbert spaces $\mathcal{H}_j$ and feature maps $\varphi_j : \mathcal{X} \to \mathcal{H}_j$. We are interested in finding the mixing weights $\beta_j \geq 0$, $j = 1, \dots, m$, that result in the best SVM classifier with a kernel of the form

$$k(x, x') = \sum_{j=1}^{m} \beta_j k_j(x, x'). \tag{10.2}$$

[2] *Kernel target alignment* has also been applied to the problem of learning linear kernel combinations, see *e.g.* [Lanckriet et al., 2004]. However multiple kernel learning has been found to yield better results for practical applications.

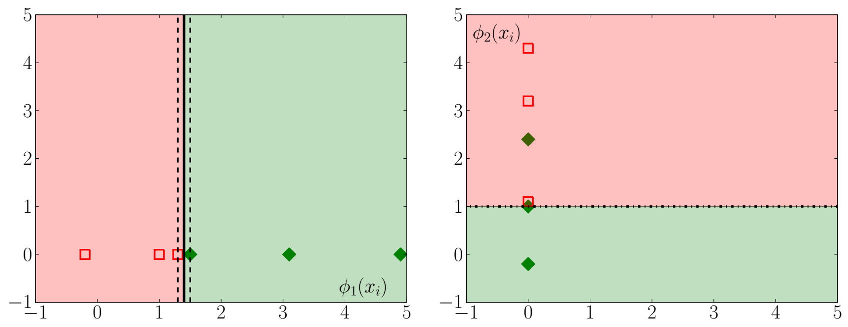

(a) Left: using the representation $\varphi_1(x_i)$ the classification problem is solvable only with very small margin. Right: using the representation $\varphi_2(x_i)$ the data points are even non-separable.

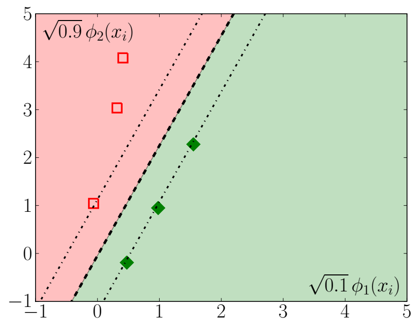

(b) Represented by a combination of φ_1 and φ_2, the dataset becomes much better separable.

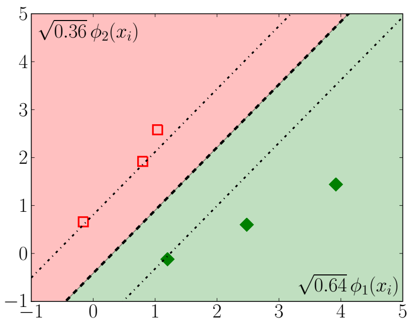

(c) A mixing coefficient of $\beta = 0.64$ leads to the maximal possible margin.

Figure 10.1 Example of multiple kernel learning. (a): given two kernels k_1 and k_2 with features maps φ_1 and φ_2, neither is well suited to solve the resulting classification problem. (b): a linear kernel combination $k(x,x') = \beta\, k_1(x,x') + (1-\beta)\, k_2(x,x')$ with induced feature map $(\sqrt{\beta}\varphi_1, \sqrt{1-\beta}\,\varphi_2)$ can result in a better linear classifier. (c): solving the optimization (10.4) we can calculate the optimal mixing coefficients.

For fixed coefficients $\beta_1, \dots, \beta_m$, we can think of k as inducing the product Hilbert space $\mathcal{H} = \mathcal{H}_1 \times \cdots \times \mathcal{H}_m$ by means of the stacked feature map $\varphi(x) = (\sqrt{\beta_1}\varphi_1(x), \dots, \sqrt{\beta_m}\varphi_m(x))$, because the scalar product induced by this construction has the same values as k:

$$\langle \varphi(x), \varphi(x') \rangle_{\mathcal{H}} = \sum_{j=1}^{m} \beta_j \langle \varphi_j(x), \varphi_j(x') \rangle_{\mathcal{H}_j} = k(x,x'). \tag{10.3}$$

By decomposing and reparameterizing the weight vector as $w =$

$(\frac{1}{\sqrt{\beta_1}}v_1, \dots, \frac{1}{\sqrt{\beta_m}}v_m)$ the SVM objective (2.33) becomes

$$\min_{\substack{(v_1,\dots,v_m)\in\mathcal{H}_1\times\dots\times H_m\\ \xi_1,\dots,\xi_n\in\mathbb{R}^+}} \sum_{j=1}^{m} \frac{1}{\beta_j}\|v_j\|_{\mathcal{H}_j^2} + \frac{C}{n}\sum_{i=1}^{n}\xi_i \tag{10.4}$$

subject to

$$y_i \sum_{j=1}^{m} \langle v_j, \varphi(x_i)\rangle_{\mathcal{H}_j} \geq 1 - \xi_i, \qquad \text{for } i = 1, \dots n. \tag{10.5}$$

In order to find the best coefficients for the linear combination kernel, we optimize (10.4) over all kernel choices, *i.e.* over $(\beta_1, \dots, \beta_m)$. However, changing β influences not only the margin, but by means of the feature map φ also the distribution of points in the feature space. Specifically, multiplying k with a constant will increase the margin, but it will also scale the point coordinates such that, geometrically, the situation is unaffected. To avoid this degenerate behavior, we bound the norm of β by either $\|\beta\|_{L^1} = 1$ (L^1-*MKL* [Bach et al., 2004]) or $\|\beta\|_{L^2} = 1$ (L^2-*MKL* [Kloft et al., 2008])[3]. The resulting optimization problem is *jointly-convex* in the vectors v_j and in the kernel coefficients β_j [Sonnenburg et al., 2006]. Consequently, there is a unique global minimum, and we can find it efficiently using standard optimization techniques. Note that in the case of an L^1 constraint, $\sum_{j=1}^{m}\beta_j = 1$, the coefficients β_j will typically become sparse, *i.e.* many β_j will be 0. This distinguishes relevant from irrelevant kernels and allows the interpretation of multiple kernel learning as a feature selection technique.

A recent extension, *infinite kernel learning* [Gehler and Nowozin, 2009b] combines the advantages of *kernel target alignment* and *multiple kernel learning*: it allows the learning of a linear kernel combination while at the same time adjusting the continuous-valued kernel parameters.

[3] Interestingly, the third natural choice, $\|\beta\|_{L^\infty} = 1$ results in the data-independent solution $\beta_1, \dots, \beta_m = 1$, *i.e.* the "best" kernel is formed by just summing all base kernels.

10.3 Example: Image Classification

G. Bakır, M. Wu and J. Eichhorn: *"Maximum-Margin Feature Combination for Detection and Categorization"*, Technical Report 2005

[Bakır et al., 2005] were the first to recognize the potential of using multiple kernel learning to find the best feature combinations for image classification tasks. They define a set of base kernels consisting of χ^2-kernels over local color histograms, Bhattacharyya-kernels for sets of SIFT features points, and Gaussian kernels for edge maps. Subsequently they learn a combined kernel for one-versus-rest SVMs with multiple kernel learning that performed better than each individual kernel in face recognition and object classification tasks.

Similar setups were later also proposed independently by [Kumar and Sminchisescu, 2007], who use MKL for object classification with different *pyramid match kernels* and *spatial pyramid kernels*, and [Varma and Ray, 2007], who rely on a variant of MKL with slightly different regularization to automatically determine the relevance of shape, color and texture features for different object classification tasks.

Note, however, that the above references show only superior performance of MKL compared to setups that use a single kernel function, but they do not compare against simpler kernel combination techniques. In fact, recent evidence by [Gehler and Nowozin, 2009a] suggests that for image classification tasks in which all base kernels reflect some relevant information, *kernel averaging* works equally well. Only if some base kernels are largely uninformative, MKL achieves superior performance.

10.4 Example: Multiclass Object Detection

C. H. Lampert and M. B. Blaschko: *"A Multiple Kernel Learning Approach to Joint Multiclass Object Detection"*, DAGM 2008

In the task of object classification in natural images, it is known that the background and the presence or absence of other object classes can be strong contextual cues. [Lampert and Blaschko, 2008] propose an MKL-based method to make use of such context. They define one base kernels for each object category to be detected as well as for the image background, and they apply MKL to learn a linear combination of these base kernels for each target class. The authors show that kernel combinations that include other object categories as context perform better than kernels based on single object regions. Additionally, the coefficients learned by MKL reflect inherent dependencies between semantically related objects groups, *e.g. animals* or *vehicles*. A similar setup has been used successfully to learn the relevance of a local neighborhood around a detection as context [Blaschko and Lampert, 2009].

Bibliography

Anguelov, D., B. Taskar, V. Chatalbashev, D. Koller, D. Gupta, G. Heitz, and A. Ng (2005), 'Discriminative learning of markov random fields for segmentation of 3D scan data'. In: *IEEE Computer Society Conference on Computer Vision and Pattern Recognition (CVPR)*. pp. 169–176.

Bach, F. R., G. R. G. Lanckriet, and M. I. Jordan (2004), 'Multiple kernel learning, conic duality, and the SMO algorithm'. In: *International Conference on Machine Learning (ICML)*.

Baird, H. S. (1993), 'Document image defect models and their uses'. In: *International Conference on Document Analysis and Recognition (ICDAR)*.

Bakır, G. H., M. Wu, and J. Eichhorn (2005), 'Maximum-margin feature combination for detection and categorization'. Technical report, Max Planck Institute for Biological Cybernetics, Tübingen, Germany.

Bay, H., T. Tuytelaars, and L. Van Gool (2006), 'SURF: Speeded up robust features'. In: *European Conference on Computer Vision (ECCV)*. pp. 404–417.

Belhumeur, P. N., J. P. Hespanha, and D. J. Kriegman (1997), 'Eigenfaces vs. fisherfaces: recognition using class specific linearprojection'. *IEEE Transactions on Pattern Analysis and Machine Intelligence (PAMI)* **19**(7), 711–720.

Belkin, M. and P. Niyogi (2003), 'Laplacian eigenmaps for dimensionality reduction and data representation'. *Neural computation* **15**(6), 1373–1396.

Ben-Hur, A., D. Horn, H. T. Siegelmann, and V. Vapnik (2002), 'Support vector clustering'. *Journal of Machine Learning Research (JMLR)* **2**, 125–137.

Bennett, K. P. and E. J. Bredensteiner (2000), 'Duality and geometry in SVM classifiers'. In: *International Conference on Machine Learning (ICML)*.

Bishop, C. M. (1995), *Neural networks for pattern recognition*. Oxford University Press, USA.

Blaschko, M. B. and C. H. Lampert (2008a), 'Correlational spectral clustering'. In: *IEEE Computer Society Conference on Computer Vision and Pattern Recognition (CVPR)*.

Blaschko, M. B. and C. H. Lampert (2008b), 'Learning to localize objects with structured output regression'. In: *European Conference on Computer Vision (ECCV)*.

Blaschko, M. B. and C. H. Lampert (2009), 'Object localization with global and local context kernels'. In: *British Machine Vision Conference (BMVC)*.

Bosch, A., A. Zisserman, and X. Munoz (2007), 'Representing shape with a spatial pyramid kernel'. In: *International Conference on Image and Video Retrieval (CIVR)*. pp. 401–408.

Boyd, S. P. and L. Vandenberghe (2004), *Convex optimization*. Cambridge University Press.

Boykov, Y. and V. Kolmogorov (2004), 'An experimental comparison of min-cut/max-flow algorithms for energy minimization in vision'. *IEEE Transactions on Pattern Analysis and Machine Intelligence (PAMI)* **26**(9), 1124–1137.

Breiman, L. (1998), *Classification and regression trees*. Chapman & Hall/CRC.

Bădoiu, M., S. Har-Peled, and P. Indyk (2002), 'Approximate clustering via core-sets'. In: *ACM Symposium on Theory of Computing*. pp. 250–

257.

Chapelle, O. (2007a), 'Training a support vector machine in the primal'. *Neural Computation* **19**(5), 1155–1178.

Chapelle, O. (2007b), 'Training a support vector machine in the primal'. *Neural Computation* **19**(5), 1155–1178.

Charikar, M., S. Khuller, D. Mount, and G. Narasimhan (2001), 'Algorithms for facility location problems with outliers'. In: *ACM SIAM Symposium on Discrete Algorithms (SODA)*. pp. 642–651.

Chen, Y., X. S. Zhou, and T. S. Huang (2001), 'One-class SVM for learning in image retrieval'. In: *IEEE International Conference on Image Processing (ICIP)*. pp. 34–37.

Crammer, K. and Y. Singer (2001), 'On the algorithmic implementation of multiclass kernel-based vector machines'. *Journal of Machine Learning Research (JMLR)* **2**, 265–292.

Cristianini, N., J. Shawe-Taylor, A. Elisseeff, and J. Kandola (2001), 'On kernel-target alignment'. In: *Advances in Neural Information Processing Systems (NIPS)*, Vol. 15. pp. 367–373.

Csurka, G., C. R. Dance, L. Fan, J. Willamowski, and C. Bray (2004), 'Visual categorization with bags of keypoints'. In: *ECCV Workshop on Statistical Learning in Computer Vision*.

Decoste, D. and B. Schölkopf (2002), 'Training invariant support vector machines'. *Machine Learning* **46**(1), 161–190.

Deselaers, T., D. Keysers, and H. Ney (2005), 'Improving a discriminative approach to object recognition using image patches'. In: *Symposium of the German Pattern Recognition Society (DAGM)*. pp. 326–335.

Dietterich, T. G. and G. Bakiri (1995), 'Solving multiclass learning problems via error-correcting output codes'. *Journal of Artificial Intelligence Research* **2**, 263–286.

Dollar, P., V. Rabaud, G. Cottrell, and S. Belongie (2005), 'Behavior recognition via sparse spatio-temporal features'. In: *IEEE International Workshop on Visual Surveillance and Performance Evaluation of Tracking and Surveillance (VS-PETS)*. pp. 65–72.

Drucker, H., C. J. C. Burges, L. Kaufman, A. Smola, and V. Vapnik (1996), 'Support vector regression machines'. In: *Advances in Neural Information Processing Systems (NIPS)*, Vol. 10. pp. 155–161.

Efron, B. and G. Gong (1983), 'A leisurely look at the bootstrap, the jackknife, and cross-validation'. *American Statistician* **37**(1), 36–48.

Fergus, R., P. Perona, and A. Zisserman (2003), 'Object class recognition by unsupervised scale-invariant learning'. In: *IEEE Computer Society Conference on Computer Vision and Pattern Recognition (CVPR)*.

Fischler, M. A. and R. A. Elschlager (1973), 'The representation and matching of pictorial structures'. *IEEE Transactions on Computers* **100**(22), 67–92.

Forman, G. (2003), 'An extensive empirical study of feature selection metrics for text classification'. *Journal of Machine Learning Research (JMLR)* **3**, 1289–1305.

Fukumizu, K., A. Gretton, X. Sun, and B. Schölkopf (2008), 'Kernel measures of conditional dependence'. In: *Advances in Neural Information Processing Systems (NIPS)*, Vol. 22. pp. 489–496.

Gehler, P. and S. Nowozin (2009a), 'Feature combination methods for kernel classifiers'. In: *IEEE International Conference on Computer Vision (ICCV)*.

Gehler, P. and S. Nowozin (2009b), 'Let the kernel figure it out; principled learning of pre-processing for kernel classifiers'. In: *IEEE Computer Society Conference on Computer Vision and Pattern Recognition (CVPR)*.

Girolami, M. (2002), 'Mercer kernel-based clustering in feature space'. *IEEE Transactions on Neural Networks* **13**(3), 780–784.

Grauman, K. and T. Darrell (2005), 'The pyramid match kernel: discriminative classification with sets of image features'. In: *IEEE International Conference on Computer Vision (ICCV)*. pp. 1458–1465.

Gusfield, D. (1997), *Algorithms on strings, trees, and sequences*. Cambridge University Press, New York.

Haasdonk, B. and H. Burkhardt (2007), 'Invariant kernel functions for pattern analysis and machine learning'. *Machine Learning* **68**(1), 35–61.

Harris, C. and M. Stephens (1988), 'A combined corner and edge detector'. In: *Alvey Vision Conference*. pp. 147–151.

Hein, M. and O. Bousquet (2005), 'Hilbertian metrics and positive definite kernels on probability measures'. In: *International Conference* *on Artificial Intelligence and Statistics (AISTATS)*.

Hiemstra, D. (2000), 'A probabilistic justification for using tf×idf term weighting in information retrieval'. *International Journal on Digital Libraries* **3**(2), 131–139.

Hinton, G. E., S. Osindero, and Y. W. Teh (2006), 'A fast learning algorithm for deep belief nets'. *Neural Computation* **18**(7), 1527–1554.

Horst, R. and N. V. Thoai (1999), 'DC programming: overview'. *Journal of Optimization Theory and Applications* **103**(1), 1–43.

Hotelling, H. (1936), 'Relations between two sets of variates'. *Biometrika* **28**(3-4), 321–377.

Hsu, C. and C. Lin (2002), 'A comparison of methods for multiclass support vector machines'. *IEEE Transactions on Neural Networks* **13**(2), 415–425.

Jiang, Y. G., C. W. Ngo, and J. Yang (2007), 'Towards optimal bag-of-features for object categorization and semantic video retrieval'. In: *International Conference on Image and Video Retrieval (CIVR)*. pp. 494–501.

Joachims, T. (2006), 'Training linear SVMs in linear time'. In: *ACM International Conference on Knowledge Discovery and Data Mining (KDD)*. pp. 217–226.

Jolliffe, I. T. (1986), 'Principal component analysis'. *Springer, New York*.

Kloft, M., U. Brefeld, P. Laskov, and S. Sonnenburg (2008), 'Non-sparse multiple kernel learning'. In: *NIPS Workshop on Kernel Learning: Automatic Selection of Optimal Kernels*.

Kohavi, R. (1995), 'A study of cross-validation and bootstrap for accuracy estimation and model selection'. In: *International Joint Conference on Artificial Intelligence (IJCAI)*. pp. 1137–1145.

Kumar, A. and C. Sminchisescu (2007), 'Support kernel machines for object recognition'. In: *IEEE International Conference on Computer Vision (ICCV)*.

Kwok, J. T. Y. and I. W. H. Tsang (2004), 'The pre-image problem in kernel methods'. *IEEE Transactions on Neural Networks* **15**(6), 1517–1525.

Lafferty, J. D., A. McCallum, and F. C. N. Pereira (2001), 'Conditional random fields: probabilistic models for segmenting and labeling sequence data'. In: *International Conference on Machine Learning (ICML)*. pp. 282–289.

Lai, P. L. and C. Fyfe (2000), 'Kernel and nonlinear canonical correlation analysis'. *International Journal of Neural Systems* **10**(5), 365–378.

Lampert, C. H. and M. B. Blaschko (2008), 'A multiple kernel learning approach to joint multi-class object detection'. In: *Symposium of the German Pattern Recognition Society (DAGM)*. pp. 31–40.

Lampert, C. H., M. B. Blaschko, and T. Hofmann (2008), 'Beyond sliding windows: object localization by efficient subwindow search'. In: *IEEE Computer Society Conference on Computer Vision and Pattern Recognition (CVPR)*.

Lampert, C. H., M. B. Blaschko, and T. Hofmann (2009), 'Efficient subwindow search: a branch and bound framework for object localization'. *IEEE Transactions on Pattern Analysis and Machine Intelligence (PAMI)*.

Lanckriet, G. R. G., N. Cristianini, P. Bartlett, L. El Ghaoui, and M. I. Jordan (2004), 'Learning the kernel matrix with semidefinite programming'. *Journal of Machine Learning Research (JMLR)* **5**, 27–72.

Lazebnik, S., C. Schmid, and J. Ponce (2006), 'Beyond bags of features: spatial pyramid matching for recognizing natural scene categories'. In: *IEEE Computer Society Conference on Computer Vision and Pattern Recognition (CVPR)*. pp. 2169–2178.

Li, Y., S. Gong, J. Sherrah, and H. Liddell (2004), 'Support vector machine based multi-view face detection and recognition'. *Image and Vision Computing* **22**(5), 413–427.

Linden, A. and J. Kindermann (1989), 'Inversion of multilayer nets'. In: *International Joint Conference on Neural Networks (IJCNN)*. pp. 425–430.

Loupias, E., N. Sebe, S. Bres, and J. M. Jolion (2000), 'Wavelet-based salient points for image retrieval'. In: *IEEE International Conference on Image Processing (ICIP)*. pp. 518–521.

Lowe, D. G. (2004), 'Distinctive image features from scale-invariant keypoints'. *International Journal of Computer Vision (IJCV)* **60**(2), 91–110.

Lyu, S. and H. Farid (2004), 'Steganalysis using color wavelet statistics and one-class support vector machines'. In: *SPIE Symposium on Electronic Imaging*. pp. 35–45.

MacQueen, J. (1967), 'Some Methods for Classification and Analysis of Multivariate Observations'. In: *Fifth Berkeley Symposium on Mathematics, Statistics and Probability*, Vol. 1. pp. 281–296.

McLachlan, G. J. (1992), *Discriminant analysis and statistical pattern recognition*. Wiley New York.

Mika, S., G. Rätsch, J. Weston, B. Schölkopf, and K. R. Müller (1999), 'Fisher discriminant analysis with kernels'. In: *IEEE Workshop on Neural Networks for Signal Processing*. pp. 41–48.

Mikolajczyk, K. and C. Schmid (2004), 'Scale and affine invariant interest point detectors'. *International Journal of Computer Vision (IJCV)* **60**(1), 63–86.

Mundy, J. L. and A. Zisserman (1992), *Geometric invariance in computer vision*. MIT Press Cambridge, MA, USA.

Nene, S. A., S. K. Nayar, and H. Murase (1996), 'Columbia Object Image Library (COIL-100)'. Technical report, Department of Computer Science Columbia University, New York.

Nowak, E., F. Jurie, and B. Triggs (2006), 'Sampling strategies for bag-of-features image classification'. In: *European Conference on Computer Vision (ECCV)*. pp. 490–503.

Nowozin, S., G. Bakır, and K. Tsuda (2007), 'Discriminative subsequence mining for action classification'. In: *IEEE International Conference on Computer Vision (ICCV)*.

Odone, F., A. Barla, and A. Verri (2005), 'Building kernels from binary strings for image matching'. *IEEE Transactions on Image Processing* **14**(2), 169–180.

Platt, J. C. (1999), 'Fast training of support vector machines using sequential minimal optimization'. In: *Advances in Kernel Methods: Support Vector Learning*. MIT Press, pp. 185–208.

Platt, J. C., N. Cristianini, and J. Shawe-Taylor (1999), 'Large margin DAGs for multiclass classification'. In: *Advances in Neural Informa-*

tion Processing Systems (NIPS), Vol. 13. pp. 547–553.

Quadrianto, N., L. Song, and A. J. Smola (2008), 'Kernelized sorting'. In: *Advances in Neural Information Processing Systems (NIPS)*, Vol. 22.

Quinlan, J. R. (1986), 'Induction of decision trees'. *Machine Learning* **1**(1), 81–106.

Rasmussen, C. E. and C. Williams (2006), *Gaussian processes for machine learning*. MIT Press.

Rényi, A. (1959), 'On measures of dependence'. *Acta Mathematica Hungarica* **10**(3), 441–451.

Rifkin, R. and A. Klautau (2004), 'In defense of one-vs-all classification'. *Journal of Machine Learning Research (JMLR)* **5**, 101–141.

Saunders, C., A. Gammerman, and V. Vovk (1998), 'Ridge regression learning algorithm in dual variables'. In: *International Conference on Machine Learning (ICML)*. pp. 515–521.

Schapire, R. and Y. Freund (1997), 'A decision theoretic generalization of on-line learning and an application to boosting'. *Journal of Computer and System Sciences* **55**(1), 119–139.

Schölkopf, B., C. Burges, and V. Vapnik (1995), 'Extracting support data for a given task'. In: *ACM International Conference on Knowledge Discovery and Data Mining (KDD)*. pp. 252–257.

Schölkopf, B., J. C. Platt, J. Shawe-Taylor, A. J. Smola, and R. C. Williamson (2001), 'Estimating the support of a high-dimensional distribution'. *Neural Computation* **13**(7), 1443–1471.

Schölkopf, B. and A. J. Smola (2002), *Learning with kernels*. MIT Press.

Shalev-Shwartz, S., Y. Singer, and N. Srebro (2007), 'Pegasos: Primal Estimated sub-GrAdient SOlver for SVM'. In: *International Conference on Machine Learning (ICML)*. pp. 807–814.

Shawe-Taylor, J. and N. Cristianini (2004), *Kernel methods for pattern analysis*. Cambridge University Press.

Sietsma, J. and R. J. F. Dow (1991), 'Creating artificial neural networks that generalize'. *Neural Networks* **4**(1), 67–79.

Simard, P., Y. LeCun, J. S. Denker, and B. Victorri (1999), 'Transformation invariance in pattern recognition – tangent distance and tangent propagation'. In: *Neural Networks: Tricks of the Trade*. Springer, pp. 239–274.

Sivic, J. and A. Zisserman (2003), 'Video google: a text retrieval approach to object matching in videos'. In: *IEEE International Conference on Computer Vision*. pp. 1470–1477.

Smith, J. R. and S. F. Chang (1996), 'Tools and techniques for color image retrieval'. In: *Storage and Retrieval for Image and Video Databases (SPIE)*. pp. 426–437.

Sonnenburg, S., G. Rätsch, C. Schäfer, and B. Schölkopf (2006), 'Large scale multiple kernel learning'. *The Journal of Machine Learning Research* **7**, 1531–1565.

Swain, M. J. and D. H. Ballard (1991), 'Color indexing'. *International Journal of Computer Vision (IJCV)* **7**(1), 11–32.

Szummer, M., P. Kohli, and D. Hoiem (2008), 'Learning CRFs using graph cuts'. In: *European Conference on Computer Vision (ECCV)*. pp. 582–595.

Taskar, B., C. Guestrin, and D. Koller (2003), 'Max-margin markov networks'. In: *Advances in Neural Information Processing Systems (NIPS)*, Vol. 17.

Tax, D. M. J. and R. P. W. Duin (2004), 'Support vector data description'. *Machine Learning* **54**(1), 45–66.

Tipping, M. and B. Schölkopf (2001), 'A kernel approach for vector quantization with guaranteed distortion bounds'. In: *Artificial Intelligence and Statistics (AISTATS)*. pp. 129–134.

Tsochantaridis, I., T. Joachims, T. Hofmann, and Y. Altun (2005), 'Large margin methods for structured and interdependent output variables'. *Journal of Machine Learning Research (JMLR)* **6**, 1453–1484.

Turk, M. and A. Pentland (1991), 'Eigenfaces for recognition'. *Journal of Cognitive Neuroscience* **3**(1), 71–86.

Tuytelaars, T., C. Lampert, M. Blaschko, and W. Buntine (2009), 'Unsupervised object discovery: a comparison'. *International Journal of Computer Vision (IJCV)*.

Tuytelaars, T. and K. Mikolajczyk (2008), 'Local invariant feature detectors: a survey'. *Foundations and Trends in Computer Graphics and Vision* **3**(3), 177–280.

Vapnik, V. N. (1998), *Statistical learning theory*. Wiley.

Varma, M. and D. Ray (2007), ‘Learning the discriminative power-invariance trade-off’. In: *IEEE International Conference on Computer Vision (ICCV)*.

Wallraven, C., B. Caputo, and A. Graf (2003), ‘Recognition with local features: the kernel recipe’. In: *IEEE International Conference on Computer Vision (ICCV)*. pp. 257–264.

Weston, J., A. Elisseeff, B. Schölkopf, and M. Tipping (2003), ‘Use of the zero norm with linear models and kernel methods’. *Journal of Machine Learning Research (JMLR)* **3**, 1439–1461.

Wood, J. (1996), ‘Invariant pattern recognition: a review’. *Pattern Recognition* **29**(1), 1–17.

Yang, M. (2002), ‘Kernel eigenfaces vs. kernel fisherfaces: Face recognition using kernel methods’. In: *IEEE International Conference on Automatic Face and Gesture Recognition*. pp. 215–220.

Young, R. A. (1987), ‘The Gaussian derivative model for spatial vision: I. Retinal mechanisms’. *Spatial Vision* **2**(4), 273–293.

Zhang, J., M. Marszalek, S. Lazebnik, and C. Schmid (2007), ‘Local features and kernels for classification of texture and object categories: a comprehensive study’. *International Journal of Computer Vision (IJCV)* **73**(2), 213–238.